

THE UNIVERSITY OF CHICAGO

BMP9 MODULATES ADULT HIPPOCAMPAL NEUROGENESIS

A DISSERTATION SUBMITTED TO
THE FACULTY OF THE DIVISION OF THE BIOLOGICAL SCIENCES
AND THE PRITZKER SCHOOL OF MEDICINE
IN CANDIDACY FOR THE DEGREE OF
DOCTOR OF PHILOSOPHY

COMMITTEE ON GENETICS, GENOMICS, AND SYSTEMS BIOLOGY

BY

MARY ROSE ROGERS

CHICAGO, ILLINOIS

DECEMBER 2017

TABLE OF CONTENTS

LIST OF TABLES.....	iii
LIST OF FIGURES.....	iv
LIST OF ABBREVIATIONS	v
ACKNOWLEDGEMENTS.....	viii
CHAPTER 1: INTRODUCTION.....	1
CHAPTER 2: BMP9 MODULATES ADULT HIPPOCAMPAL NEUROGENESIS.....	20
CHAPTER 3: CONCLUSION.....	45
APPENDIX: SUPPLEMENTARY TABLES AND FIGURES.....	57
REFERENCES.....	64

LIST OF TABLES

Table A.1.	Primer sequences for genotyping <i>Bmp9</i> KO mice.....	57
Table A.2.	Antibodies used for multilabel immunohistochemistry.....	58
Table A.3.	Primers used for qPCR.....	59

LIST OF FIGURES

Figure 1.1.	Lineage progression and timeline of neural development in the adult hippocampus.....	4
Figure 2.1.	Proliferation of early progenitors is reduced in <i>Bmp9</i> KO mice.....	31
Figure 2.2.	<i>Bmp9</i> KO mice do not have an altered distribution of early precursors and astrocytes.....	32
Figure 2.3.	Deregulation of neural precursors does not decrease the success of neuronal lineage commitment in <i>Bmp9</i> KO mice.....	35
Figure 2.4.	Survival of new-born neurons is transiently enhanced in <i>Bmp9</i> KO mice.....	36
Figure 2.5.	Endogenous BMP9 is not necessary for cholinergic support in the medial septum and the diagonal band of Broca.....	38
Figure A.1	Gene targeting strategy for generation of <i>Bmp9</i> KO mice.....	60
Figure A.2	Experimental design for thymidine analog pulse labeling and multi-label immunostaining.	61
Figure A.3	<i>Bmp9</i> KO mice do not exhibit signs of hypervascularization.....	62
Figure A.4	<i>Bmp9</i> is not expressed in the adult male mouse brain.....	63

LIST OF ABBREVIATIONS

AD	Alzheimer's Disease, an age-related neurodegenerative disease
ActR	Activin Receptor, a type of TGF β superfamily receptor
ALK	Activin-receptor like kinase, a type I TGF β superfamily receptor
AMPA	α -amino-3-hydroxyl-5-methyl-4-isoxazole-propionate, a specific agonist for the AMPA receptor
Ascl1	Achaete-scute complex homolog 1, a member of the bHLH family of transcription factors
AVM	Arteriovenous malformation
BDNF	Brain-derived neurotrophic factor
BMP	Bone Morphogenetic Protein
BMPR	Bone Morphogenetic Protein Receptor
BrdU	5-bromo-2-deoxyuridine, a synthetic thymidine analogue commonly used for the detection of in vivo proliferating cells
CA1	Cornu Ammonis 1 subregion of the hippocampal formation
CA3	Cornu Ammonis 3 subregion of the hippocampal formation
ChAT	Choline acetyltransferase
DAPI	4',6-diamidino-2-phenylindole; intercalates between nucleotide bases to stain cell nuclei
DCX	Doublecortin, a protein expressed in migrating immature neurons
DG	Dentate Gyrus, subregion of the hippocampal formation and site of ongoing
EC	Endothelial cell
GABA	γ -Aminobutyric acid, a neurotransmitter
GC	Granule Cell

GCL	Granule Cell Layer, a subregion of the dentate gyrus or olfactory bulb
GFAP	Glial Fibrillary Acid Protein, an intermediate filament protein that is found in glial cells such as astrocyte as well as radial glial cells
GFP	Green Fluorescent Protein, commonly used to label proteins or cells
Hes5	Hairy and enhancer of split 5
HHT	Hereditary hemorrhagic telangiectasia
bHLH	Basic Helix-Loop-Helix, a protein structural motif that characterized a family of transcription factors
Id	Inhibitor of DNA binding
IGF	Insulin-like growth factor
Ki67	A protein expressed during cell cycle and used as a marker for proliferating cells
KO	Knockout
LTP	Long-term potentiation
NeuN	Neuronal Nuclei, a neuron-specific nuclear antigen, a specific marker for neuronal protein
NGF	Nerve Growth Factor
NKCC1	A sodium-potassium-chloride cotransporter
NMDA	N-methyl-D-aspartic acid, an amino acid derivative agonist of NMDA receptors
NSC	Neural Stem Cell
hNSC	horizontal Neural Stem Cell
OB	Olfactory Bulb
PFA	paraformaldehyde
SGZ	Sub Granular Zone, subregion of the dentate gyrus in the hippocampal Formation

Sox2	The transcription factor Sry-related homeobox (HMG-box) 2, used as a marker of neural stem cells and embryonic stem cells.
SVZ	Subventricular Zone; region lining the lateral walls of the lateral ventricles and site of ongoing neurogenesis throughout adulthood
TGF β	Transforming Growth Factor Beta
Tbr2	T-box brain protein 2
TrKA	Neurotrophic Tyrosine Kinase A
VEGF	Vascular Endothelial Growth Factor, a subfamily of a platelet-derived growth factor family and a signaling protein involved in angiogenesis
Wnt	A large family of signaling proteins embryonic and adult neurogenesis, among other roles
Wt	Wild-type

ACKNOWLEDGMENTS

I would first like to thank my advisor and mentor Tong-Chuan He for his guidance and encouragement throughout my time in graduate school. He challenged me to continuously reach beyond my knowledge and motivated me to strive for the most rigorous science. He has been generous with his time and his support of my project, always making an effort to discuss results and to determine the direction forward. I have benefited greatly from his passion for scientific inquiry, a passion I hope to take forward in my own career.

I am also extremely grateful to my thesis committee members, Chip Ferguson, Daniel Peterson, Brian Popko, Clifton Ragsdale, and Gopal Thinakaran. I feel privileged to have had the opportunity to benefit from their experience and expert knowledge as well as their guidance and support. I am very grateful to Chip Ferguson for having introduced me to the topic of adult neurogenesis my first quarter of graduate school. I am eternally thankful for Daniel Peterson and his generosity. He has given me so much: time, knowledge, resources, and hope. I am thankful for Brian Popko, who is kind enough to act as Committee Chairman and always gives sound advice and has moved me forward along my path. I am very grateful to Clifton Ragsdale for sharing his vast background and expertise in development, which allowed me to see my project from another exciting view point. I am also very thankful for Gopal Thinakaran, an expert in Alzheimer's disease, who also gave invaluable advice throughout our meetings. Together, they have provided me with encouragement and granted me insight. I am forever grateful to them all. I would also like to thank members of the He Lab and Peterson Lab for all of their assistance and training. I would especially like to thank Qiang Wei, Zach Collier, and Zari Dumanian for all

their help with animal work. In the Peterson Lab, I am especially grateful for Sarah Schuck for training me when she was nine months pregnant. And I will always be thankful I had the best lab-mate, Stanley Bazarek. In addition, I would like to thank the Chairman of the GGSB, Yoav Gilad. We could not ask for anyone better to guide us. I am also so very fortunate for Sue Levison, the Administrator of the GGSB, who treats all with so much love and care.

Finally, I would like to thank the love of my life, John Jakubowski, for his undying support through everything.

CHAPTER 1

INTRODUCTION

ADULT HIPPOCAMPAL NEUROGENESIS

Neurogenic Regions In The Adult Mammalian Brain

Adult neurogenesis occurs in two specialized regions of the mammalian brain under physiological conditions: i) the subventricular zone (SVZ), which is located in the lateral ventricles, and ii) the subgranular zone (SGZ) of the dentate gyrus (DG), which is located in the hippocampus. In the rodent brain, newborn neurons generated in the SVZ migrate along astrocytes to the olfactory bulb (OB). In the OB, they differentiate into interneurons that subsequently replace those previously integrated into the network (Gage, 2000; Ming and Song, 2011). In humans, SVZ neurogenesis sharply declines within the first year and the physiological significance is not well understood. By contrast, the structure and connectivity of the hippocampus is conserved between humans and rodents and adult neurogenesis continues throughout life in both species. During adult hippocampal neurogenesis, newborn neurons in the SGZ migrate only a short distance into the granular cell layer (GCL) as they differentiate into mature granule cells (GCs), the principal cell of the dentate gyrus. Rather than replace existing neurons, newly generated neurons are incorporated into the existing hippocampal circuitry (Kempermann et al., 2015).

Despite striking differences in niche organization, neuroblast migration, and production of neuronal subtypes, the stages of adult neurogenesis in the SVZ and SGZ are marked by the same set of developmental milestones: neural stem cell (NSC) activation, progenitor

proliferation, generation of neuroblasts, changes in electrophysical properties, synaptic integration, and functional maturation of newly generated neurons (Gage, 2000; Ming and Song, 2011). This sequence of events recapitulates the process of neuronal development in embryonic and postnatal brains and is similarly orchestrated by overlapping sets of transcription factors (Hodge et al., 2012). The signaling pathways regulating adult neurogenesis and developmental neurogenesis are similarly conserved, but the source of signaling molecules and cellular response vary among neurogenic regions. In the SVZ/OB and SGZ, adult neurogenesis occurs in the pre-existing niche microenvironment and signaling factors are produced by a variety of terminally differentiated cell types, including astrocytes, endothelial cells, and fully mature neurons (Ming and Song, 2011). Within the niche microenvironment, combinatorial input and signal integration confer permissiveness and facilitate dynamic modulation of adult neurogenesis (Gonçalves et al., 2016). By contrast, in the embryonic brain neurogenesis and gliogenesis are temporally segregated and local signaling occurs in the broader context of morphogenesis. Recently, it has been suggested that adult NSCs share the same core machinery with their embryonic counterparts and that modulatory mechanisms repurpose individual components to accommodate unique aspects of adult neurogenesis, namely long-term maintenance of NSCs and dynamic tuning of neurogenic output in response to environmental stimuli (Götz et al., 2016). While this idea has not been formally tested, it underscores the importance of the niche microenvironment. Likewise, it calls attention to the question of whether age-related reductions in neurogenesis are caused by loss of a permissive signaling in the niche or intrinsic changes in NSCs.

Adult Hippocampal Neurogenesis: Stages Of Neuronal Development

Adult hippocampal neurogenesis comprises a sequence of progressive morphological and electrophysical changes that culminate in the production of new granule cells in the DG. As the

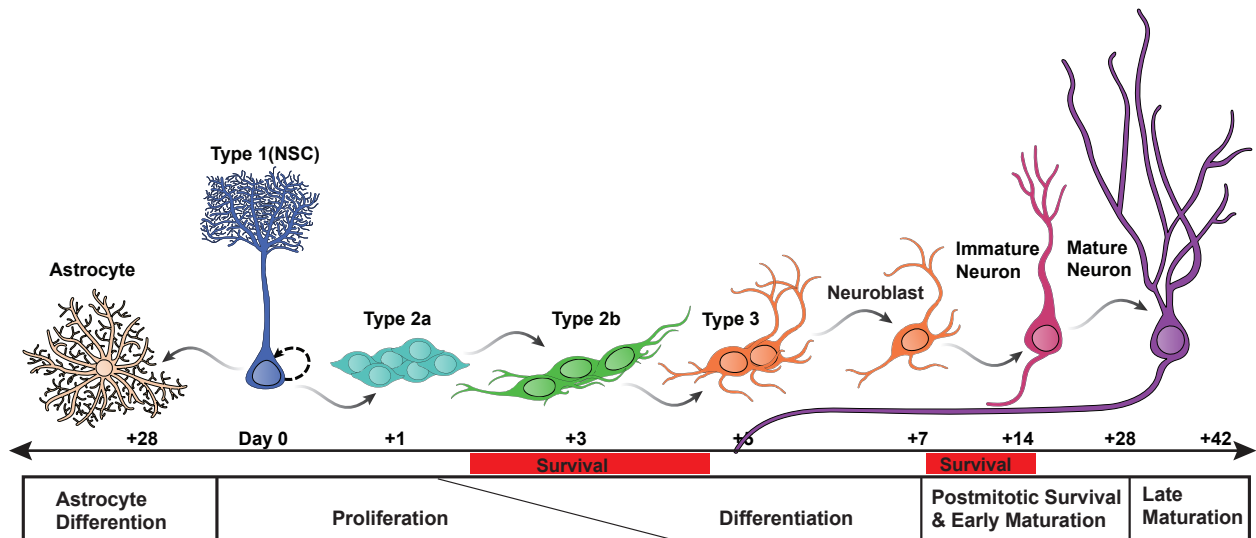
precursor from which all others arise, adult hippocampal NSCs are often referred to as Type 1 cells and are typically represented by radial glia-like cells (RGLs). Type 1 cells generate Type 2 cells, which are divided into Type 2a and Type 2b subpopulations, the latter of which give rise to Type 3 cells (neuroblasts). Type 3 cells exit the cell cycle and give rise to newborn, immature neurons that subsequently mature into functional granule cells (Fig. 1.1). In contrast to embryonic neurogenesis, where the magnitude of neurogenic output is set to a fixed developmental endpoint, neuronal development in the SGZ is dynamically modulated at all stages and in response to a variety of environmental stimuli. The number of new neurons generated in the adult brain is thus determined by the additive effects of precursor proliferation, successful commitment to the lineage, post-mitotic survival, activity-dependent recruitment, and maturation of newborn neurons (Kempermann et al., 2015).

The precursor cell phase: neural stem cells

The continual generation of new neurons throughout life is fundamentally dependent on the population NSCs (RGLs/Type 1 cells) residing in the SGZ of the dentate gyrus (DG). RGLs/Type 1 cells express Nestin, glial fibrillary acid protein (GFAP), and Sry-related homeobox 2 (SOX2) and have a characteristic apical process that traverses the granule cell layer (GCL) and forms dense arborizations in the inner molecular layer of the DG (Bonaguidi et al., 2012; Lagace et al., 2007; Seri et al., 2001). Though RGLs/Type 1 cells are primarily quiescent, this complex morphology facilitates regulatory interactions from multiple sources and the ability to be mobilized in response to specific stimuli (Lugert et al., 2010; Moss et al., 2016). Utilizing Nestin-CreER^{T2} mice for inducible and sparse labeling in vivo clonal analysis, it was shown individual RGLs/Type 1 cells shuttle between quiescent and active states and vary with regard to

Figure 1.1. Lineage progression and timeline of neural development in the adult hippocampus.

Type 1 cells are multipotent neural stem cells (NSCs) that develop into new neurons and astrocytes in the SGZ. Through asymmetric division, Type 1 cells both self-renew and produce an intermediate progenitor cell. Within the neurogenic lineage, there are three types of intermediate progenitor cells (IPCs). These populations undergo progressive rounds of symmetric cell division and differentiation to amplify the neural precursor population. Most of these cells undergo apoptosis. Progenitor cells that survive complete differentiation within one week. Over the following three weeks new-born cells acquire morphological features of mature neurons. Neurogenic output is dependent on combinatorial regulation of progenitor proliferation, differentiation, survival, and maturation. Continual generation of new neurons throughout life is associated with maintenance of the NSC pool. The production of new astrocytes similarly depends on Type 1 NSCs. Following cell-cycle exit, post-mitotic Type 1 cells differentiate into astrocyte progenitors. In contrast to IPCs of the neurogenic lineage, astrocyte progenitors have restricted proliferation. Similar to IPCs, astrocytes progenitors are successfully differentiated into astrocytes within one week and reach maturation by 4 weeks.



capacity for self-renewal and fate potential. Once activated, RGLs/Type 1 cells are faced with four choices: divide symmetrically to expand the population, divide asymmetrically to self-renew and generate a progenitor of either neuronal or glial fate, or terminally differentiate into astrocytes (Bonaguidi et al., 2011).

In addition to RGLs/Type 1 cells, a second set of SOX2⁺ neural precursors with stem cell-like properties has been identified. These cells, referred to as nonradial SOX2⁺ precursors, lack the characteristic apical process of RGLs/Type 1 cells and have short, horizontal processes (Suh et al., 2007). In vivo lineage analysis has shown nonradial SOX2⁺ cells maintain SOX2 expression at least one month after cell division, proliferate in response to running, and serve as precursors for both neurons, astrocytes, and possibly RGLs/Type 1 cells (Suh et al., 2007). In terms of morphology, marker expression, and behavior, nonradial SOX2⁺ neural precursors share characteristics with Type 2a cells, a more differentiated precursor cell type.

On the basis of Notch dependency, Lugert et al. used Hes5::GFP mice to label the subpopulation of nonradial SOX2⁺ cells with stem-cell like characteristics, referred to as horizontal neural stem cells (hNSCs). Using Hes5::GFP mice, Lugert et al. characterized the behavior of RGLs/Type 1 cells and hNSCs under basal conditions, during aging, and in response to running and kainite-induced seizures (Lugert et al., 2010). Under basal conditions, RGLs/Type 1 cells are mostly quiescent and hNSCs serve as the primary neural precursor. During aging, there is a proportionate decrease in proliferative activity in both populations and hNSCs thus account for the age-associated decrease in neurogenesis, whereas seizures activate both cell types, but primarily expand the population of hNSCs. By contrast, RGLs/Type 1 cells are specifically mobilized in response to physical activity and undergo asymmetric cell division, thus increasing the total number of RGLs and hNSCs without changing the relative proportion of

the two subpopulations (Lugert et al., 2010).

The precursor cell phase: type 2 and type 3 intermediate progenitor cells

To prevent exhaustive cycling, hippocampal NSCs generate Type 2 cells, a population of proliferative intermediate progenitor cells (IPCs). Type 2 cells divide to expand the precursor pool and are responsive to stimuli that modulate neuronal output. Type 2 cells are divided into Type 2a and Type 2b subpopulations on the basis of glial and neuronal markers, respectively. Type 2a cells express SOX2 and high levels of the proneural gene Achaete-scute complex homolog 1 (*Ascl1*). As Type 2a cells differentiate into Type 2b cells, expression of the transcription factor T-box brain protein 2 (Tbr2) is upregulated. Tbr2 binds to the promoter of *Sox2* to downregulate expression and is believed to drive neuronal commitment (Hodge et al., 2012). Consistent with this idea, only a small proportion of SOX2⁺ cells also express Tbr2. By contrast, the majority of Tbr2⁺ cells co-label with NeuroD1 and doublecortin (DCX), a lineage marker for neuronal commitment (Hodge et al., 2008). As Type 2b cells differentiate into Type 3 cells, expression of NeuroD1 and DCX persists and Tbr2 is downregulated. Approximately half of the newly generated Type 2 cells undergo apoptosis at the Type 2b cell stage, which marks the first critical point for cell survival. The transition of Type 2b cells to Type 3 cells, also referred to as neuroblasts, determines the number of successfully committed neuronal precursors. At the Type 3 cell stage, expression of NeuroD1 and DCX persists, whereas Tbr2 is suppressed (Hodge et al., 2008).

While the majority of newly generated Type 2 cells either undergo apoptosis or become successfully committed Type 3 cells, Type 2a and Type 2b cells can also be pushed into quiescence by local signaling factors (Bond et al., 2014; Lugert et al., 2010; 2012). In response

to various environmental stimuli, such as running and environmental enrichment, quiescent Type 2 cells can be reactivated for lineage amplification. As neurogenesis is initiated at a later stage of neuronal development, reactivation of Type 2 cells accelerates the tempo of progenitor maturation as a population-based effect (Bond et al., 2014). Although this mechanism facilitates rapid generation of immature neurons, an appropriate stimulus for activity-dependent recruitment, such as learning, is required for long-term survival (Bond et al., 2014; Kempermann et al., 1997).

In the traditional model of adult hippocampal neurogenesis, RGLs/Type 1 cells divide asymmetrically to generate a highly proliferative Type 2a cell. Through progressive rounds of symmetric cell division, Type 2a cells expand the neural precursor pool before differentiating into Type 2b cells. In turn, Type 2b cells undergo relatively fewer cell divisions and give rise to Type 3 progenitors that rarely divide. In this model, referred to as the IP-driven model of homeostatic neurogenesis, newborn neurons are generated in two weeks and are morphologically mature by four weeks. By contrast, the stem-cell and early neuroblast-driven model of homeostatic neurogenesis indicates precursor expansion occurs through proliferation of hNSCs and Type 2b cells. In this model, it requires over three weeks to generate Type 3 cells and several more weeks before maturation is complete. As newborn neurons can take several weeks to mature into neurons, they are poised for both adaptive responses and fine-tuned integration into the circuitry (Lugert et al., 2012). Importantly, as precursor proliferation and activity-dependent recruitment are temporally segregated, newborn neurons might serve as a “cognitive reserve” to sustain plasticity under circumstances where proliferation of NSCs or Type 2 cells is diminished, such as aging (Kempermann, 2015; Lugert et al., 2012).

Similar to models of neural stem cell behavior, it is likely the dynamics of IP-driven neurogenesis versus stem-cell and early neuroblast-driven neurogenesis are not mutually exclusive, but rather demonstrate different aspects of the same process. Likewise, discrepancies between these two models seem to arise, at least in part, by differences in labeling techniques and delineation of Type 2a cells and hNSCs. For example, as hNSCs are not identified in the IP-driven model, the shorter amount of time to generate newborn neurons, i.e. two weeks versus three weeks in the stem-cell and early neuroblast-driven neurogenesis model, may be due to labeling a more differentiated cell type. Alternatively, as the IP-driven model is largely constructed from lineage analysis of RGLs and hNSCs serve as the primary precursor under homeostatic conditions, it is conceivable the dynamics of Type 2 and Type 3 cell behavior observed in the two models are a consequence of originating from different NSC subpopulations.

Selective survival and postmitotic maturation

Neurogenic lineage advancement is marked by changes in electrophysical properties that facilitate survival and synaptic integration of newborn neurons. At the early precursor stage, cells express high levels of the NKCC1, a chloride importer, and GABA is depolarizing. By the Type 2b cell stage, precursors begin to receive synaptic inputs from GABAergic interneurons in the hilus and activation transitions from tonic to phasic. GABA remains depolarizing after Type 3 cells exit the cell cycle (Ge et al., 2006). As neuronal development proceeds, newborn neurons receive glutamatergic input and NKCC1 is replaced by KCC2, the latter resulting in GABAergic transmission to a switch from depolarizing to hyperpolarizing (Ge et al., 2006). These electrophysical changes are essential for proper neuronal development and activity-dependent recruitment into the preexisting circuitry (Tashiro et al., 2007; 2006; van Praag et al., 2002).

During the period of postmitotic maturation, newborn neurons undergo a number of morphological changes that facilitate synaptic integration. Dendrites extend toward the molecular layer and form complex arbors, while axons project toward CA3 (Ge et al., 2006; Markakis and Gage, 1999; Plümpe et al., 2006; Zhao et al., 2006). Axonal projections from newborn neurons reach their appropriate targets and establish functional synapses with CA3 pyramidal cells, mossy cells, and hilar interneurons within three weeks of their birth (Markakis and Gage, 1999; Toni et al., 2008). By approximately four weeks immature neurons are morphologically mature, but are hyperexcitable and have enhanced synaptic plasticity in comparison to those from previous generations. Enhanced synaptic plasticity continues until approximately six weeks and defines a critical period for newly generated neurons to make unique contributions to the pre-existing circuitry (Ge et al., 2007).

Regulation Of Adult Hippocampal Neurogenesis

The microenvironment of the dentate gyrus is crucial for maintaining neurogenic capacity and mediating adaptive responses to physiologic and pathological stimuli. In addition to neurogenic subtypes and mature neurons, cellular components of the niche include astrocytes, microglia, endothelial cells from the proximal vasculature, and afferents projecting from neurons residing in other regions of the brain (Ming and Song, 2011). Together, these cells provide a unique complement of extracellular signaling factors that is dynamically tuned by environmental stimuli. As cells advance through the stages of neuronal development, the changes in morphology, electrophysical properties, and receptor profile facilitate a variety of signaling outcomes from different cell types exposed to the same combination of signaling factors. Differential regulation on the basis of signal convergence allows dynamic modulation while

simultaneously conferring robustness to the ever-changing composition of signaling factors within the niche environment (Gonçalves et al., 2016). Importantly, the response elicited by a particular cell type in the adult brain often differs from that of its embryonic counterpart and the overall effect on neurogenesis is often different (Götz et al., 2016).

Adult hippocampal neurogenesis is modulated by neurotransmitters from hippocampal network activity, i.e. GABA and glutamate, as well as those from other regions of the brain, such as acetylcholine, dopamine, and serotonin. In addition, several signaling pathways that regulate developmental processes also modulate neuronal development in the adult dentate gyrus, including Hedgehog, Notch, Wnt, and bone morphogenetic protein (BMP) signaling pathways. As a characteristic feature of niche signaling, many of these ligands confer differential modulation among neurogenic cell types and mediate dynamic responses (Gonçalves et al., 2016). As described below, BMP signaling and RGL/Type 1 cells are particularly suited to illustrate these points in the context of environmental stimuli and niche maintenance.

The type I receptors BMPR1A (also known as activin receptor-like kinase 3, ALK3) and BMPR1B (also known as ALK6), and the cognate BMP type II receptor, BMPRII, are expressed on cells throughout the SGZ and GCL of the dentate gyrus (Charytoniuk et al., 2000; Söderström et al., 1996). BMPR1A is expressed by quiescent RGLs/Type 1 cells and is progressively downregulated as the cell approaches proliferative status. By contrast, BMPR1B expression progressively increases as cells advance through the lineage. Abrogating BMP signaling in RGLs/Type 1 cells through either blockade of BMPR1A or using administration of Noggin, a BMP antagonist, leads to activation and a subsequent exhaustion of the neural stem cell pool (Mira et al., 2010). Congruent with the pattern of BMPR1B expression, BMP signaling also regulates the balance of quiescence and activation in more differentiated precursors (Bond et al.,

2014; Mira et al., 2010). In the SGZ of adult mice, conditional deletion of *Bmpr2* in *Ascl1*-positive neural precursors, i.e. nonradial SOX2+/Type 2a cells, resulted in recruitment into the lineage and expansion of newborn neurons (Bond et al., 2014). Taken together, RGLs/Type 1 cells and other neural precursor cell populations appear to be differentially regulated through the use of BMPR1A and BMPR1B. Although BMP signaling balances activation and quiescence in both cell types, the consequences for tissue homeostasis and function are diametrically opposed.

RGLs/Type 1 cells contact the vasculature in the SGZ and ensheath blood vessels in the molecular layer (Licht and Keshet, 2015; Moss et al., 2016). These interactions facilitate bidirectional signaling between RGLs/Type 1 cells and specialized endothelial cells (ECs) for coordinated regulation of vascular endothelial growth factor (VEGF)-induced angiogenic-neurogenic coupling (Cao et al., 2004; Goldman and Chen, 2011; Palmer et al., 2000; Vivar et al., 2013). Similar to RGLs/Type 1 cells, ECs are mostly quiescent under basal conditions, but are activated in response to physical activity or hypoxic injury (Fabel et al., 2003; Goldman and Chen, 2011; Rafii et al., 2016). Importantly, activation of *Noggin* expression increases in the dentate gyrus during exercise, thus demonstrating the need to antagonize BMP-mediated quiescence for RGL/Type 1 cell activation and the appropriate response to physiological stimulus for neurogenesis (Bond et al., 2014; Gobeske et al., 2009; Lugert et al., 2010; Mira et al., 2010; van Praag et al., 1999). In contrast, decreased RGL/Type 1 cell activation is a hallmark of aging and is associated with increased levels of BMP in the hippocampus (Gonçalves et al., 2016). Recently, it has been suggested the physical interactions between the vasculature and RGLs/Type 1 cells might be to facilitate niche homeostasis (Licht and Keshet, 2015; Moss et al., 2016; Rafii et al., 2016). Demonstrating the importance of the vasculature in niche homeostasis and adult neurogenesis, studies utilizing heterochronic parabiosis have

provided evidence that factors in young blood rejuvenate neural vasculature, increase neurogenesis, enhance synaptic plasticity, and improve cognitive function in aging mice (Katsimpardi et al., 2014; Villeda et al., 2014). Taken together, these findings provide a conceptual framework for dynamic modulation.

BMP9 FUNCTION IN CONTEXT

The TGF β /BMP Signaling Pathway

The transforming growth factor (TGF)-Beta (TGF β) superfamily comprises over 30 structurally related signaling molecules from four subfamilies: Activins/Inhibins, TGF β , Bone Morphogenetic Proteins (BMPs), and Growth and Differentiation Factors (GDFs) (Mueller and Nickel, 2012). Collectively, TGF β members regulate numerous developmental and homeostatic processes in multiple organs (Harradine and Akhurst, 2006; Horbelt et al., 2012). TGF β ligands are secreted as dimers and signal through heterotetrameric complexes composed of two serine/threonine kinase receptor subtypes, type I and type II (Wrana et al., 1994; Yamashita et al., 1994). In mammals there are a total of seven type I receptors, ALK1–7, and five type II receptors. Different ligands bind to different combinations of type I and type II receptors, but the signaling mechanism is fundamentally the same among all TGF β members (Mueller, 2015). Upon ligand binding, the constitutively activate type II receptor phosphorylates the type I receptor in a highly conserved glycine and serine (GS) rich domain (de Caestecker, 2004; Mueller, 2015; Saitoh et al., 1996; Wieser et al., 1995; Willis et al., 1996; Wrana et al., 1994). Activated type I receptors provide a binding site for receptor-associated SMADS (R-SMADS), which are divided into two groups on the basis of type I receptor specificity (Chen et al., 1996; Feng and Derynck, 1997; Kretschmar et al., 1997; Liu et al., 1996; Nakao et al., 1997). The

first group is phosphorylated by ALK1, ALK2, ALK3, and ALK6 and includes SMAD1, SMAD5, and SMAD8 (SMAD1/5/8). The second group is phosphorylated by ALK4, ALK5, and ALK7 and includes SMAD2 and SMAD3 (SMAD2/3) (Mueller, 2015). Once phosphorylated, R-SMADS oligomerize and form complexes with SMAD4, the common mediator (Co-SMAD) for all R-SMADs. SMAD complexes translocate to the nucleus to modulate expression of TGF β target genes (Mueller, 2015; Zhang et al., 1996).

With almost 20 members, BMPs and GDFs form the largest subgroup of TGF β ligands. On the basis of sequence homology and function, BMP and GDF ligands can be further organized into seven different groups: BMP2/4; BMP5/6/7/8; GDF5/6/7; BMP9 (GDF2)/BMP10; GDF1/3; GDF10/BMP3; GDF9/BMP15; and GDF8/11 (Mueller and Nickel, 2012). Consistent with the traditional division of TGF β signaling into TGF β and BMP pathways, the majority of BMP and GDF ligands (BMP2/4/5/6/7/8/9/10; GDF5/6/7) bind type I receptors associated with SMAD1, SMAD5, and SMAD8 (Graff et al., 1996; Mueller and Nickel, 2012). Within this subgroup, type I receptors are highly promiscuous and ligand specificity is limited (Mueller and Nickel, 2012). For example, whereas only BMP9 and BMP10 bind with high affinity to ALK1, the majority of BMPs interact with ALK3 and ALK6 (David et al., 2007; Heinecke et al., 2009; Mueller and Nickel, 2012). Of note, GDF8 and GDF11 activate SMAD2 and SMAD3 downstream of ALK4 and ALK5 (Mueller, 2015; Rebbapragada et al., 2003). In addition, *sensu stricto* TGF β s activate both SMAD1/5/8 and SMAD2/3 downstream of ALK1 and ALK5, respectively (Mueller, 2015; Orlova et al., 2011). With regard to type II receptor subtypes, BMP and GDF ligands interact with BMPRII, ACTRII, and ACTRIIB (Mueller, 2015; Townson et al., 2012). Similar to type I receptors, type II receptors are also highly promiscuous (Mueller, 2015). In the context of temporal and spatial overlap of multiple

signaling components, the landscape of receptor-ligand interactions is determined by relative differences in binding affinity.

To increase multi-functionality, TGF β ligands can also activate non-canonical signaling pathways. Those specific to BMPs signal through BMPRII to differentially activate SMAD-mediated and mitogen activating protein kinase (MAPK) p38 by binding in a step-wise manner to type I and type II complexes or to those that are preformed (Nohe et al., 2002). This mechanism is associated with receptor internalization through clatherin coated pits or caveolae and signaling from endosomes (Hartung et al., 2006). BMP receptors can form complexes with the MAP kinase kinase kinase TAK1 (TGF β -activated kinase 1) and its activator, TAB1, via the ubiquitin ligase X-chromosome-linked inhibitor of apoptosis protein (XIAP) (Yamaguchi et al., 1999). In addition, BMPRII associates with the LIM-domain-containing protein kinase 1 (LIMK1), which is important for actin stabilization and neurite outgrowth (Eaton and Davis, 2005; Foletta et al., 2004; Matsuura et al., 2007).

BMP9: Physiological Context And Mechanisms

The response elicited by a particular ligand can be altered by other mechanisms, including processing of the prodomain, formation of the receptor complex, and signaling through non-canonical pathways. To elicit context-specific responses, TGF β signaling is regulated at multiple levels. At the cell surface, soluble and membrane-bound proteins modulate ligand binding and receptor activation (Mueller, 2015; Rider and Mulloy, 2010). Among the soluble BMP/GDF antagonists relevant to BMP9 are Noggin and Crossveinless 2 (CV2) (Seemann et al., 2009; Yao et al., 2012). BMP9, BMP10, and GDF5 are the only BMP/GDFs that are not inhibited by Noggin (Seemann et al., 2009). By contrast, BMP9 induces expression of CV2 for BMP9 inhibition through negative feedback (Yao et al., 2012). Among the membrane bound

proteins, the auxiliary receptor Endoglin has high affinity for BMP9 and can sensitize cells to BMP9 activation when ALK1 expression is low (Saito et al., 2017).

Angiogenesis

BMP9 binds with high affinity to ALK1, a TGF β receptor predominately expressed on endothelial cells (ECs), and is most commonly described as an antiangiogenic factor (David et al., 2007; Seki et al., 2003). BMP9 was shown to strongly inhibit sprouting angiogenesis in the mouse sponge assay and inhibited blood circulation in the chicken chorioallantoic membrane assay (David et al., 2008). BMP9 is predominately expressed in the liver and is present at physiologically relevant levels in both mouse and human plasma during postnatal development and throughout adulthood (Bidart et al., 2012). As a circulating factor, BMP9 gains access and binds to ALK1 and Endoglin expressed on the luminal side of ECs (Ricard et al., 2010; Saito et al., 2017). Mutations in ALK1 and Endoglin are associated with abnormalities in vascular development that serve as the basis for hereditary hemorrhagic telangiectasia (HHT) (Dupuis-Girod et al., 2010; Shovlin et al., 1997). HHT vascular lesions are characterized by direct arteriovenous connections without an intervening capillary bed. Smaller lesions, telangiectasias, are typically localized in mucosal membranes, whereas larger arteriovenous malformations (AVMs) are found in the brain, lung, and liver. The formation of these lesions is associated with hypervascularization that results from loss of ALK1 signaling observed in animal models retinal angiogenesis.

Angiogenesis is a multistep process that involves coordinated interactions between ECs and growth factors in the local microenvironment. Once activated, specialized ECs form sprouts and grow outward until connecting with other nascent vessels. At the leading edge, endothelial tip cells extend filopodia and guide migration in response to environmental cues, whereas

adjacent stalk cells trail behind to form the lumen and stabilize the nascent vessel. Evidence suggests BMP9-ALK1 signaling functions as an antiangiogenic factor by modulating VEGF responsiveness and promoting the stalk cell phenotype in cooperation with the NOTCH signaling pathway (Larrivée et al., 2012). VEGFR2 is highly expressed in tip cells and activation by VEGF promotes expression of DLL4. In turn, DLL4 binds to NOTCH receptors on adjacent cells and induces expression of canonical target genes *Hes1*, *Hey1*, and *Hey2*, as well as *Jag1*. NOTCH pathway effectors decrease VEGF signaling by downregulating transcription of VEGFR2 and VEGFR3, and upregulating VEGFR1, a decoy receptor (Larrivée et al., 2012). Decreasing VEGF sensitivity drives stalk cell fate by downregulating expression of *Dll4*, whereas JAG1 interacts with DLL4 in cis on the stalk cell membrane to antagonize NOTCH signaling in adjacent tip cells. BMP9-ALK1 signaling also induces *Hes1*, *Hey1*, and *Hey2* and thus synergizes with NOTCH to promote stalk cell fate over tip cell specification (Larrivée et al., 2012). BMP9-ALK1 signaling has been shown to suppress VEGF expression through SMAD1 (Shao et al., 2009). The BMP9-ALK1-ID1/ID3 signaling axis also induces expression of EphrinB2 (Kim et al., 2012). EphrinB2 modulates the duration and intensity of VEGF signaling through internalization of VEGFR2 and VEGFR3 and is required for proper angiogenesis and lymphangiogenesis (Nakayama et al., 2013; Sawamiphak et al., 2010; Wang et al., 2010).

During embryonic development, BMP9 and BMP10 have partially overlapping expression patterns and the two ligands are functionally equivalent for vascular development, i.e. BMP10 can compensate for loss of BMP9 (Chen et al., 2013; Ricard et al., 2012). However, functional redundancy between the two ligands is incomplete and dependent on physiological context. Analysis of *Bmp9*^{10/10} mice, where *Bmp10* has been replaced with *Bmp9*, demonstrated BMP10 has a role in cardiac development that cannot be compensated for by BMP9 (Chen et al.,

2013). Conversely, *Bmp9* missense mutations have been recently associated with vascular abnormalities that overlap with HHT, thus demonstrating that circulating BMP9 is required for vascular homeostasis in adults (Wooderchak-Donahue et al., 2013).

Bmp9 promotes differentiation and maintenance of cholinergic neurons

Bmp9 is expressed in the CNS during embryonic and postnatal development and in the aging adult brain. Lopez-Coviella et al. demonstrated *Bmp9* is expressed in the septal region at E14, a developmental time point that corresponds to a period of cholinergic differentiation (Lopez-Coviella, 2000). Treatment of E14 septal cultures with BMP9 increased expression of choline acetyltransferase (ChAT) and vesicular acetylcholine transporter (vAChT), which are required for synthesis of acetylcholine (ACh), the neurotransmitter of cholinergic neurons. When injected into the cerebral ventricles at E14 and E16, BMP9 increased levels of ACh in the forebrain (Lopez-Coviella, 2000). BMP9 also induces the expression of other genes belonging to the transcriptome of septal cholinergic neurons, suggesting the function of BMP9 in cholinergic development is not limited to neurotransmitter synthesis (Lopez-Coviella et al., 2005). BMP9 also induced genes encoding proteins that modulate trophic support, including nerve growth factor (NGF) and TrkA (the high affinity receptor for NGF). Of note, BMP9-induced expression of NGF was restricted to p75-positive basal forebrain cholinergic neurons (BFCN), the only septal cells shown to express ALK1 (Schnitzler et al., 2010). Accordingly, it has been suggested that BMP9 promotes cholinergic development by increasing trophic support prior to target innervation (Schnitzler et al., 2010).

Evidence suggests that BMP9 also has a neuroprotective effect on fully mature BFCN. When administered to adult mice subjected to fimbria fornix transection (a lesion which

abrogates trophic support from post-synaptic neurons), BMP9 is able to maintain the cholinergic phenotype of the severed neurons (Lopez-Coviella et al., 2011). In addition, *Bmp9* is expressed in the brains of aging mice and might be required to prevent age-related diminishments in BFCN function and cholinergic marker expression or mitigate the effects of neurodegenerative disease (Mellott et al., 2014). Providing support for this idea, intracerebroventricular infusions of BMP9 decreased amyloidosis and the cholinergic defect in APP.PS1 mice, a transgenic mouse model of Alzheimer's disease (Mellott et al., 2014). Intracerebroventricular delivery of IGF2 similarly reduced amyloidosis in APP.PS1 mice and also increased the level of BMP9 protein in the hippocampus. Interestingly, IGF2 also increased DCX protein, suggesting an increase in adult neurogenesis (Burke et al., 2013).

Taken together, multiple studies have demonstrated BMP9 is sufficient to promote differentiation and maintenance of BFCN. To date, however, whether endogenous BMP9 is necessary for these processes has not been determined.

PROJECT OVERVIEW

BMP9 is a circulating factor and well-established regulator of angiogenesis, lymphangiogenesis, and promotes cholinergic function in a number of contexts. As a circulating factor, BMP9 gains access to the somatic stem cell niche of multiple organs. Here, we examine the regulatory potential of BMP9 in adult hippocampal neurogenesis. The project can be summarized in two primary goals: 1) assess neural stem cell and progenitor dynamics and 2) examine survival of newborn neurons.

To detect and quantify stage-specific alterations in neuronal development, we combined thymidine analog pulse-labeling, multi-label immunofluorescence, and design-based stereology.

Our experimental design employed two different pulse-labeling schemes corresponding to each one of the goals: the first was to detect changes in proliferation, whereas the second was to evaluate selective survival. This approach allowed us to identify significant differences within both precursor and post-mitotic stages of the neuronal lineage. We show proliferation is specifically decreased in the Type 2a progenitor population, but an increase in the number of label-retaining immature neurons in *Bmp9KO* mice. These findings demonstrate loss of BMP9 causes dysregulation of the neurogenic process and defines a new role for BMP9.

CHAPTER 2

BMP9 MODULATES ADULT HIPPOCAMPAL NEUROGENESIS

ABSTRACT

Adult hippocampal neurogenesis continually produces new granule cells in the dentate gyrus. The capacity to generate new neurons throughout life is fundamentally dependent on maintaining a reservoir of neural stem cells and the integrity of the neurogenic niche. Within the niche, endothelial cells function as intermediary signaling platforms that modulate neurogenesis in response to circulating factors and bidirectional communication with adjacent neural stem cells. Adult neurogenesis decreases with age and is paralleled by vascular deterioration and cognitive decline. These changes are associated with a loss of circulating factors that have not yet been identified. Here, we show loss of bone morphogenetic protein 9 (BMP9), a circulating factor required for vascular homeostasis, alters the dynamics of adult hippocampal neurogenesis. Thymidine analog pulse-labeling revealed proliferative activity is specifically decreased in Type 2a cells in *Bmp9*KO mice. Surprisingly, despite this loss in progenitor amplification, the number of cells successfully committed to the neuronal lineage is comparable between the two groups. In *Bmp9*KO mice, label retention is increased in immature neurons, suggesting reduced proliferation in *Bmp9*KO mice is mitigated by an increase in cell survival. In addition, we show *Bmp9* is not expressed in the brain at the age neurogenesis was examined, thus precluding cell-

autonomous regulation of neurogenic populations as previously reported for other BMPs. Taken together, these observations demonstrate BMP9 has a modulatory function in homeostatic neurogenesis.

INTRODUCTION

Adult neurogenesis occurs in two specialized regions of the mammalian brain under physiological conditions: i) the subventricular zone (SVZ), which is located in the walls of the lateral ventricles, and ii) the subgranular zone (SGZ) of the dentate gyrus, which is located in the hippocampus (Doetsch et al., 1997; Gage, 2000; Seri et al., 2004). The capacity to generate new neurons throughout life is fundamentally dependent on the population of adult neural stem cells (NSCs) and the uniquely permissive environment of the neurogenic niche (Gage, 2000). Within these specialized microenvironments, cells interact with each other and the proximal vasculature through a network of physical contacts and extracellular signals (Licht and Keshet, 2015; Palmer et al., 2000; Seri et al., 2004). This cellular crosstalk facilitates dynamic regulation of proliferation, differentiation, maturation, and survival of neural precursors and new-born neurons (van Praag et al., 2002). The process of adult hippocampal neurogenesis comprises a sequence of progressive morphological and electrophysical changes that culminate in the production of new granule cells in the dentate gyrus (Ge et al., 2006; Tashiro et al., 2006; 2007; van Praag et al., 2002; Zhao et al., 2006). These changes mark developmental milestones and are represented by six cell types (Kempermann et al., 2004). As the precursor from which all others arise, NSCs are often referred to as Type 1 cells and are typically represented by radial glia-like cells (RGLs). Type 1 cells generate Type 2 cells, which are divided into Type 2a and Type 2b subpopulations (also referred to as intermediate progenitors, IPCs), the latter of which give rise to Type 3 cells

(neuroblasts). Type 3 cells exit the cell cycle and give rise to newborn, immature neurons that subsequently mature into functional granule cells. The number of new neurons generated is modulated by precursor proliferation, which expands the neurogenic population, successful commitment to the lineage, and selective survival during the period of post-mitotic maturation. By adding new neurons to the hippocampal circuitry, neurogenesis provides the cellular basis for neuronal plasticity and is crucial for learning and adaptive behavior (Ge et al., 2007).

In addition to being a site for neurogenesis, the dentate gyrus also undergoes changes in the vasculature through angiogenesis (Cao et al., 2004; Goldman and Chen, 2011; Palmer et al., 2000; Vivar et al., 2013). Blood vessels serve as conduits for oxygen and nutrient delivery, as well as a source of angiocrines secreted from specialized endothelial cells (Rafii et al., 2016). Angiocrines regulate stem and progenitor cell behavior to maintain organ homeostasis and regeneration (Rafii et al., 2016). Within the dentate gyrus, Type 1 cells (radial glia-like cells, RGLs) are the prototypic NSC. Type 1 cells have a characteristic apical process that traverses the granule cell layer and forms dense arborizations in the molecular layer that ensheath blood vessels (Licht and Keshet, 2015; Moss et al., 2016). These interactions facilitate bidirectional signaling between RGLs/Type 1 cells and angiogenic ECs for coordinated regulation of VEGF-induced angiogenic-neurogenic coupling in response to physical activity and hypoxia (Fabel et al., 2003; 2009; Goldman and Chen, 2011). Under basal conditions, however, Type 1 cells and ECs are mostly quiescent and it has been proposed these two cell types interact primarily to maintain niche homeostasis (Licht and Keshet, 2015; Moss et al., 2016).

The hippocampal vasculature is particularly vulnerable to age-related changes, which lead to compromised blood brain barrier (BBB) integrity, decreased blood perfusion, diminished adult neurogenesis, and ultimately risk for cognitive impairment (Montagne et al., 2015).

Heterochronic parabiosis studies have demonstrated a causal link between hippocampal dysfunction and age-related changes in circulating factors. The aging systemic milieu mediates a negative influence on cognitive function in young mice, partly through an increase in inflammatory cytokines (Villeda et al., 2011). By contrast, factors in young blood were shown to rejuvenate neural vasculature, increase neurogenesis, enhance synaptic plasticity, and improve cognitive function in aging mice (Katsimpardi et al., 2014; Villeda et al., 2014). Together these findings have raised interest in manipulating ‘pro-age’ and ‘pro-youth’ factors as part of a therapeutic strategy to combat aging and induce hippocampal rejuvenation (Fan et al., 2017). To date, however, the only ‘pro-youth’ factor to be identified, GDF11, is marred by controversy and the identities of circulating ‘pro-youth’ factors remain elusive (Katsimpardi et al., 2014).

BMP9 is expressed in the liver and secreted into the bloodstream during postnatal development and up to at least one year in adults. As a circulating factor, BMP9 gains access to BMP receptors expressed on the luminal side of endothelial cells, including ALK1 and Endoglin (Bidart et al., 2011; Ricard et al., 2010). During vascular development, BMP9 and BMP10 signal through ALK1 to decrease VEGF responsiveness in angiogenic endothelial cells and the two ligands are functionally equivalent in this context (Bidart et al., 2011; Chen et al., 2013; David et al., 2008). Mutations in ALK1 and Endoglin are associated with abnormalities in vascular development that serve as the basis for hereditary hemorrhagic telangiectasia (HHT) (Shovlin et al., 1997). HHT vascular lesions are characterized by direct arteriovenous connections without an intervening capillary bed. Smaller lesions, telangiectasias, are typically localized in mucosal membranes, whereas larger arteriovenous malformations (AVMs) are found in the brain, lung, and liver. Mutations in BMP9 were recently identified as the molecular lesions underlying a vascular anomaly syndrome that partially phenocopies HHT, but also has

features of capillary malformation (CM)-AVM syndrome, a group of RASA-1 related disorders. The BMP9 associated vascular anomalies thus demonstrate a unique function for circulating BMP9 in vascular homeostasis, but the sequelae and mechanisms of the BMP9 mutations are not well characterized (Wooderchak-Donahue et al., 2013).

In addition to its potential activity as a circulating factor, BMP9 might also influence adult hippocampal neurogenesis through cholinergic neurons in the basal forebrain. Basal forebrain cholinergic neurons (BFCN), innervate the hippocampus and provide modulatory input through the neurotransmitter acetylcholine (ACh). BFCN from the medial septum and diagonal band of Broca provide synaptic input to newborn neurons in the DG (Vivar et al., 2012). Conversely, denervation of BFCN with the immunotoxin 192IgG-saporin reduces survival of newborn cells and decreases neurogenic output in adult rats (Cooper-Kuhn et al., 2004). BMP9 is a potent factor sufficient to induce cholinergic differentiation and maintenance in the context of several in vitro and in vivo experimental models (Burke et al., 2013; Lopez-Coviella, 2000; Mellott et al., 2014; Schnitzler et al., 2010). BMP9 is expressed in the septal area of embryonic and postnatal brains and it has been proposed to provide trophic support prior to target innervation (Lopez-Coviella, 2000; Schnitzler et al., 2010). Likewise, BMP9 expressed in the aging brain and is sufficient to reverse BFCN degeneration in mouse models of Alzheimer's disease (AD) (Burke et al., 2013; Mellott et al., 2014). Interestingly, AD has also been associated with dysregulation of adult hippocampal neurogenesis and vascular abnormalities including capillary distortion, BBB dysfunction, and hypoperfusion (Zacchigna et al., 2008).

Extending upon the established associations between adult hippocampal neurogenesis and the previously reported functions of BMP9, namely vascular homeostasis and BFCN development and maintenance, we hypothesized BMP9 is necessary to maintain the appropriate

complement of neurogenic signaling factors derived from endothelial cells and/or cholinergic neurons for homeostatic neurogenesis. Here, we test this hypothesis using a global, constitutive *Bmp9*KO mouse to model loss-of-function. Using an unbiased stereological approach for quantitative analysis of cell populations, we examined multiple stages along the neurogenic lineage. Our results demonstrate BMP9 loss-of-function reduces proliferation of Type 2a cells and increases the survival of late-stage immature neurons. These changes, however, did not alter the total number of mature granule cells. Our findings reveal differences in population and cell dynamics that signify BMP9-mediated regulation of adult neurogenesis as mechanistically distinct from those previously described for other BMPs. These results demonstrate a previously unknown function of BMP9 in the CNS and expand our understanding of both BMP signaling and systemic regulation of adult hippocampal neurogenesis.

MATERIALS AND METHODS

Animals

Bmp9 null mutants, hereafter referred to as *Bmp9*KO, were generated in the Transgenic Core Facility at the University of Chicago using commercially available ES cells with the *Gdf2*^{tm1(KOMP)Vlcg} allele (Regeneron) and maintained on C57B6 background. Wild-type (*Bmp9*^{+/+}) and *Bmp9*KO mice for all experimental procedures were produced from *Bmp9*^{+/-} crosses (Fig. A.1). All mice were male, between 85-100 days old at the time of first CldU injection. All mice were housed in groups of 2–4 mice per cage with food and water ad libitum.

Genotyping

For genomic DNA, tail biopsies were incubated in alkaline lysis buffer (.2M NaOH, 1mM EDTA) for 30 minutes at 85°C. Lysates were diluted 1:5 in molecular grade water and

used as templates for touchdown PCR (TD-PCR). Genotypes were confirmed using primers targeted for amplification of exon1, exon2, lacz, and neo. Primer names and sequences are in Table A.1.

Preparation of Thymidine Analogs

Solutions of CldU (Sigma #C-6891) were prepared at 10 mg/ml. Injections at 2.5 ml/kg resulted in a dose of 42.5 mg/kg CldU. All halogenated thymidine analog solutions were administered by intraperitoneal injection to ensure precise delivery to facilitate quantitative comparisons.

Histology

Animals were deeply anesthetized and transcardially perfused with ice cold 0.1M PO₄ followed by 4% paraformaldehyde in the same buffer. Brains were removed, post-fixed overnight in the same fixative solution, and then transferred to 30% sucrose in 0.1M PO₄ until equilibrated. Coronal sections (40 μm) were produced on a freezing sliding microtome and sections were transferred to a cryoprotectant solution and stored at -20°C until used. Sections were washed five times in Tris Buffered Saline (TBS) before being treated with 0.2N HCl for 10 minutes at 37°C to facilitate antibody access. After acid treatment, sections were neutralized in 0.1M Borate Buffer for 10 minutes. Following an additional five washes in TBS, sections were incubated in 5% donkey serum (Jackson ImmunoResearch Laboratories 017-000-121) in TBS containing 0.25% Triton X-100. Sections were stained free floating with incubation in primary antibody for 24-72 hours at 4°C. All secondary antibodies (Jackson ImmunoResearch Laboratories) were raised in donkey and conjugated to biotin, Alexa488, Alexa594, Cy3, or Alexa647. Biotinylated secondary antibodies were detected by subsequent incubation with

streptavidin conjugated to Alexa647. Nucleic acid counterstains used were DAPI (Molecular Probes #D1306) 1:1,000 or To-Pro 3 (Molecular Probes #T3675) at 1:5,000 in TBS. Primary and secondary antibodies with respective dilutions are listed in Table A.2.

Laser Scanning Confocal Microscopy

Sections were imaged on an Olympus FluoView confocal microscope equipped with a Kr/Ar laser with three lines of excitation: 488 nm, 568 nm, and 647 nm. Background settings were adjusted from examination of negative control specimens. Images of positive staining were adjusted to make optimal use of the dynamic range of detection. Figures were composed in Adobe Photoshop with minimal alteration for presentation and layout.

Stereology

Virtual tissue of each dentate gyrus and septum section were generated from stained sections by collecting a montage of z-stacks at 60x (N.A. 1.4) using an Olympus Disk Spinning confocal microscope controlled by the StereoInvestigator software (MBF Bioscience). All counting was done post-acquisition using the Optical Fractionator method. This method estimates the total number of cells from a subset that are counted within the spaces of a virtual sampling grid. The sampling grid is placed over the region of interest, ensuring uniform distances of counting frames and systematic random sampling (SRS) during counting procedures. All cell counts were obtained under standard rules of the optical dissector. Briefly, all counting parameters used a guard zone of at least 2 microns. The optical section at the start point was used as a lookup section, and the remaining optical sections were used as reference sections. All cells were counterstained with DAPI and the top of the nucleus was used as a

unique point. All nuclei cut through the lookup section, touching an exclusion line, or outside the frame were not counted; nuclei cut exclusively through the reference sections, and touching an inclusion line or entirely within the frame were counted. Estimates were derived from the Optical Fractionator equation and CE (Coefficient of Error) values were determined within the framework of StereoInvestigator (MBF Bioscience).

RNA Isolation

Animals were deeply anesthetized and transcardially perfused with ice cold DEPC-PBS to remove blood. To evaluate endogenous *Bmp9* expression, brains were collected from wild-type mice and dissections for hippocampi, anterior, and posterior regions were performed. Wild-type livers were collected from mice and used as a positive control. Samples from *Bmp9*KO hippocampi and liver were used as negative controls. Hippocampi were collected from additional wild-type and *Bmp9*KO mice to evaluate differential gene expression. Tissue was snap frozen and stored at -80° C until RNA isolation. Total RNA was isolated with the TRIZOL Reagents RNA isolation protocol (Invitrogen). The isolated RNA was subjected to reverse transcription with hexamer and M-MuLV reverse transcriptase (New England Biolabs, Ipswich, MA). The resultant cDNA products were kept at -80° C and used as PCR templates.

Touchdown qPCR (TqPCR)

All qPCR reactions were designed and carried out according to the MIQE guidelines (Taylor et al., 2010). The PCR primers used in this study were designed by using the web-based Primer3Plus program. TqPCR was carried out using CFX-Connect, and the 2x SsoFast qPCR Supermix with EvaGreen or iTaq Universal SYBR Green Supermix. TqPCR reactions were carried out in triplicate using the following conditions: 95°C × 3' for one cycle; 95°C × 20",

66°C × 10", for 4 cycles by decreasing 3°C per cycle; 95°C × 20", 55°C × 10", 70°C × 1", followed by plate read, for 40 cycles. Serial dilutions of cDNA samples were performed to determine amplification efficiency for each primer pair. No template controls (NTCs) were used as negative controls. Primers sequences used are listed in Table A.3.

RESULTS

BMP9 Loss-Of-Function Reduces Proliferation Of Type 2a Progenitor Cells

Because dysregulation of neurogenesis often manifests in precursor populations, we first asked whether loss of *Bmp9*KO affects proliferation in the SGZ. To identify mitotic cells, we used CldU, a halogenated thymidine analog that is incorporated into DNA during S-phase. Wild-type and *Bmp9*KO mice were pulsed three times at two hour intervals and sacrificed two hours after the last injection. To detect subtype specific changes, we combined immunostaining for CldU (using a BrdU antibody) with lineage specific markers (Fig. A.2A). As proliferation under homeostatic conditions occurs at much lower levels in comparison to experimental conditions with a neurogenic stimulus, e.g. running, and neural precursor behavior is modulated by multiple signaling pathways, we expected any statistical differences would have a small to modest effect size. To achieve the resolution to detect such differences and obtain quantitative estimates with high precision, we used design-based stereology. On the basis of pilot studies, we used 50% sampling coverage and obtained CE < 1.2 for all BrdU+ cell counts.

Using GFAP and SOX2 as endogenous markers to distinguish Type 1 (GFAP+/SOX2+) from Type 2a (GFAP-/SOX2+) cells, we first evaluated the effect of BMP9 loss-of-function on the proliferative activity of early precursors (Fig. 2.1A-E). Whereas Type 1 cells in wild-type (5707) and *Bmp9*KO (5373) groups did not differ significantly (U=9.5, wild-type [n=6],

*Bmp9*KO [n=5], p=.355, Fig. 2.1B), there were significantly fewer proliferating Type 2a cells (BrdU+/GFAP-/SOX2+) for *Bmp9*KO (1305) than for wild-type mice (1781) (U=3, wild-type [n=6], *Bmp9*KO [n=5], p=.030, Fig. 2.1C).

To determine whether *Bmp9*KO mice have fewer proliferating Type 2a cells as the result of a smaller Type 2a population and/or reduced proliferative activity within the population, we determined the percentage of labeled Type 2a cells (BrdU+/GFAP-/SOX2+) within the total Type 2a cell population (GFAP-/SOX2+) for each group. *Bmp9*KO mice demonstrated a notable, but not significant, reduction in proliferative activity relative to wild-type mice ($7.94\% \pm 1.381$, wild-type [n=6]; $11.83\% \pm 1.656$, *Bmp9*KO [n=5]; p=.113, Fig. 2.1E). The total Type 2a cell population for wild-type (18568) and *Bmp9*KO (14437) groups did not differ significantly (U=9, wild-type [n=5], *Bmp9*KO [n=6], p=.329, Fig. 2.2C). In the Type 1 cell population, there was a not a significant difference in the percentage of S-labeled cells ($4.22\% \pm 0.632$, wild-type [n=6]; $5.62\% \pm 1.563$, *Bmp9*KO [n=5]; p=.396, Fig. 2.1D) and the total number of cells within the Type 1 cell population for wild-type (5707) and *Bmp9*KO (5373) mice did not differ (U=14, wild-type [n=6], *Bmp9*KO [n=5], p=.934, Fig. 2.2B). Taken together, these data suggest the relatively smaller Type 2a population in *Bmp9*KO mice is not the result of aberrant Type 1 activation and consequent depletion of the Type 1 cell population.

As angiogenesis and neurogenesis are associated, we also quantified the proportion of unidentified BrdU+ cells (BrdU+/SOX2-/GFAP-), which is a population partly composed of endothelial cell progenitors. The proportion of BrdU+/SOX2-/GFAP- cells was not different between wild-type and *Bmp9*KO mice ($9.42\% \pm 1.46$, wild-type [n=6] ; $7.96\% \pm 1.46$, *Bmp9*KO [n=5]; p=.647, Fig. A.3A), which indicates EC hypersprouting was not occurring in *Bmp9*KO mice. In addition, immunostaining for CD31 did not reveal readily apparent structural

Figure 2.1. Proliferation of early progenitors is reduced in *Bmp9*KO mice.

(A) Three month old male wild-type and *Bmp9*KO mice were injected with CldU to label cells in S-phase according to the experimental paradigm in Figure A.2A. Coronal sections were immunostained with BrdU, SOX2, and GFAP to identify proliferating Type 1 cells (BrdU+/SOX2+/GFAP+) and proliferating Type 2a cells (BrdU+/SOX+/GFAP-). Dashed lines delineate the SGZ, arrowheads show clusters of BrdU+ cells in each panel. Note BrdU+ cells primarily colocalize with SOX2 in both groups and that *Bmp9*KO mice have fewer BrdU+ cells. (B) Quantitative analysis using design-based stereology showed the number of BrdU+ Type 1 cells is not different between wild-type and *Bmp9*KO mice, but (C) significantly fewer BrdU+ Type 2a cells in *Bmp9*KO mice. (D) The proportion of BrdU+ Type 1 cells and (E) BrdU+ Type 2a cells does not differ significantly between wild-type and *Bmp9*KO mice. Scale bar equals 50 μ m. Whiskers on boxplots represent maximum and minimum values and points represent values for individual mice. n = 6 for wild-type mice; n = 5 for *Bmp9*KO mice. Error bars on bar charts represent \pm SEM for each group. *P < 0.05.

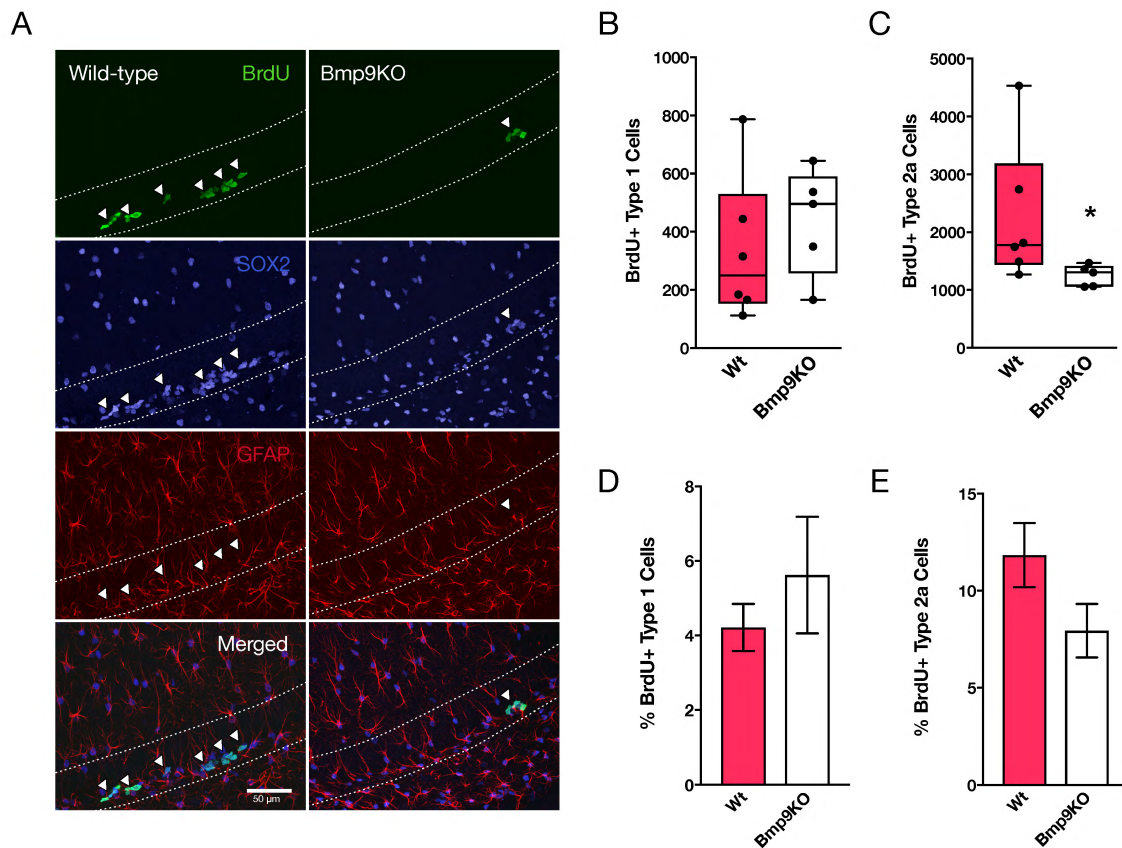
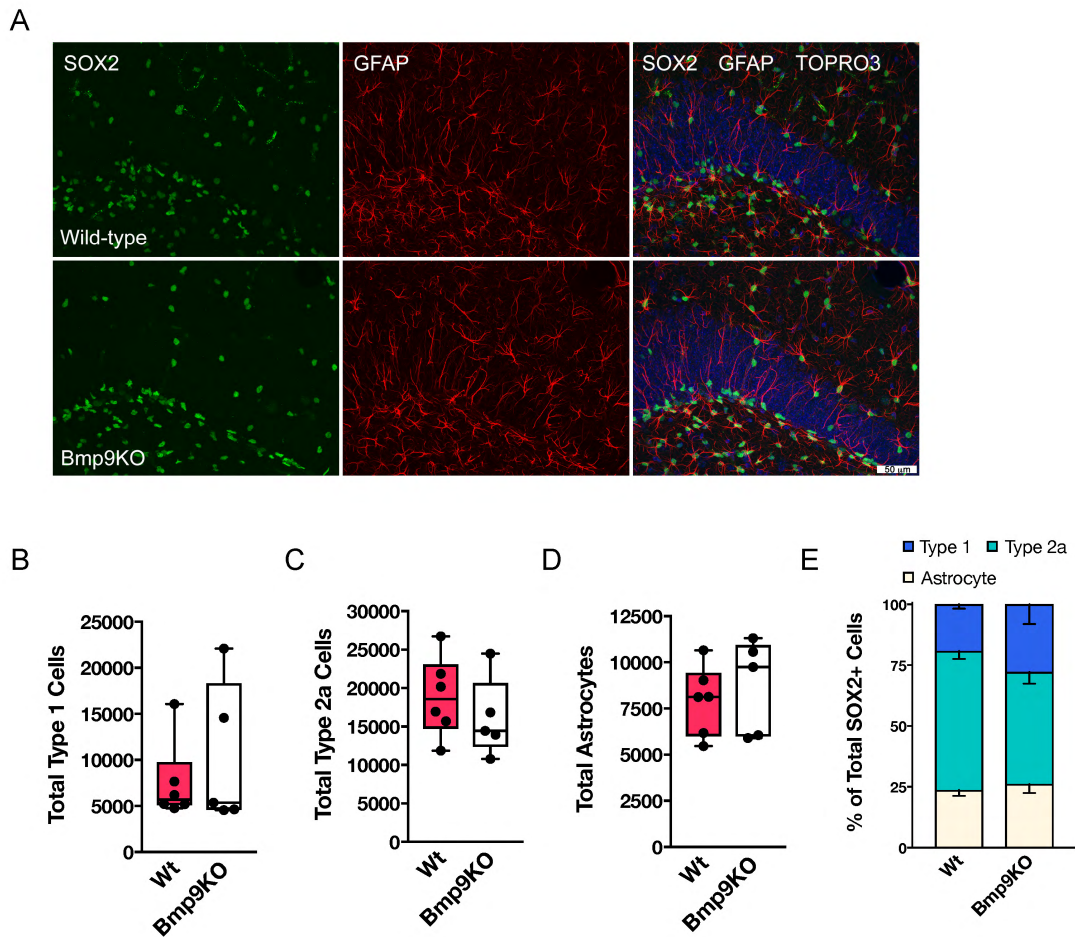


Figure 2.2. *Bmp9*KO mice do have an altered distribution of early precursors and astrocytes .

(A) Coronal sections were immunostained with SOX2 and GFAP to identify astrocytes (SOX2+/GFAP+), Type 1 cells (SOX2+/GFAP+), and Type 2a cells (SOX+/GFAP-). Astrocytes and Type 1 cells were differentiated by morphological characteristics. Note the apical processes crossing the granule cell layer, which is defined by the nuclear counterstain TOPRO3 in the merged panel of the representative image. (B-E) Quantitative analysis using design-based stereology showed the number the total number of (B) Type 1 cells, (C) Type 2a cells, and (D) astrocytes in wild-type and *Bmp9*KO mice does not differ. (E) The relative proportions of Type 1 cells, Type 2a cells, and astrocytes within the total SOX2+ population is not significantly different between wild-type and *Bmp9*KO mice. Scale bar equals 50 μ m. Whiskers on boxplots represent maximum and minimum values and points represent values for individual mice. n = 6 for wild-type mice; n = 5 for *Bmp9*KO mice. Error bars on bar charts represent \pm SEM for each group.



alterations in the vasculature of *Bmp9*KO mice (Fig. A.3B). Together, these data suggest dysregulation of Type 2a cells in *Bmp9*KO mice is not directly related to aberrant angiogenesis and that BMP9 is not required to maintain vascular quiescence under basal conditions.

Loss Of BMP9 Does Not Increase Gliogenesis

Lineage tracing of Type 1 cells has provided evidence that Type 1 cells comprise a heterogeneous population with different capacities for self-renewal and to generate neurogenic and gliogenic progeny (Bonaguidi et al., 2011). To evaluate the possibility that BMP9 alters Type 1 cell fate potential, we quantified astrocytes on the basis of morphological criteria and expression of GFAP and SOX2 (Fig. 2.2A,D). The median number of astrocytes for wild-type mice (8127) and *Bmp9*KO mice (9744) groups did not differ (U=12, wild-type [n=6], *Bmp9*KO [n=5], p=.662, Fig. 2.2D), indicating the reduction in Type 2a cell proliferation in *Bmp9*KO mice was not at the cost of astrocyte differentiation. Within the total SOX2+ population, the proportions of Type 1 cells, Type 2a cells, and astrocytes were not different between wild-type and *Bmp9*KO mice (Fig. 2.2E).

BMP9 Loss-Of-Function Does Not Alter Neuronal Lineage Commitment

Concomitant with amplifying rounds of lineage-advancing cell division, apoptosis prunes the progenitor pool (Sierra et al., 2010). Those cells that survive enter a quiescent state or differentiate into lineage-committed Type 3 cells. The transition of Type 2a progenitors into Type 2b is marked by suppression of SOX2 and upregulation of DCX, which persists until neuronal maturation is complete (Hodge et al., 2008). To evaluate the effect of BMP9 loss-of-function on Type 2b/3 progenitor proliferation and successful commitment to the neuronal

lineage, we next determined the total number of proliferating Type 2b progenitors (BrdU+/DCX+) (U=8, wild-type [n=5], *Bmp9*KO [n=5], p=.421, Fig. 2.3B), the total number of DCX+ cells (U=11, wild-type [n=5], *Bmp9*KO [n=5], p=.8413, Fig. 2.3C), and the percentage of proliferating Type 2b,3 in the total DCX+ population ($2.86\% \pm .327$, wild-type [n=5]; $2.5\% \pm .297$, *Bmp9*KO [n=5]; p=.4383, Fig. 2.3D). Small, but statistically non-significant reductions were observed in *Bmp9*KO mice for all three measurements. Combined with our findings described above, these data reveal two important points: i) BMP9 loss-of-function does not alter proliferation of Type 2b/3 progenitors and ii) Reduced proliferative capacity of Type 2a progenitors does not decrease the number of cells that are successfully committed to the neuronal lineage.

BMP9 Loss-Of-Function Enhances Survival Of Immature Neurons

The observation that the total DCX+ population in *Bmp9*KO and wild-type mice are of comparable size raises the possibility that BMP9 loss-of-function increases survival of post-mitotic cells. To investigate this possibility, we used CldU pulse-labeling to birthdate cells just prior to cell cycle exit (Fig. A.2B). Based on the timeline of lineage progression, we expected committed label-retaining-cells (LRCs) to be late stage immature neurons (BrdU+/DCX+/NeuN+) or morphologically mature neurons (BrdU+/DCX-/NeuN+) at the 23 day time point. In agreement with the idea that BMP9 loss-of-function has a pro-survival effect on postmitotic neural precursors, *Bmp9*KO mice had more label-retaining cells (LRCs) after 23 days (U=2; 377, wild-type [n=5]; 479, *Bmp9*KO [n=4], p=.0635, Fig. 2.4A). To confirm this increase of LRCs was caused by survival of neurogenic cells, we used immunostaining for DCX and NeuN to determine the total number of cells in the LRC subpopulations. *Bmp9*KO mice had

Figure 2.3. Deregulation of neural precursors does not decrease the success of neuronal lineage commitment in *Bmp9*KO mice.

(A) Three month old male wild-type and *Bmp9*KO mice were injected with CldU to label cells in S-phase according to the experimental paradigm in Figure A.2. Coronal sections were immunostained with BrdU and DCX to identify proliferating Type 2b/3 cells (BrdU+/DCX+). Note colocalization of BrdU and DCX is limited in both animals and that *Bmp9*KO mice have fewer BrdU+ cells in the representative image. (B-D) Quantitative analysis using design based stereology showed the number of (B) BrdU+ Type 2b/3 and (C) total number of DCX+ cells is not different between wild-type and *Bmp9*KO mice. (D) The relative proportion of BrdU+ Type 2b/3 to all cells committed to the neurogenic lineage is not different between wild-type and *Bmp9*KO groups. Scale bar equals 50 μ m. Whiskers on boxplots represent maximum and minimum values and points represent values for individual mice. n = 6 for wild-type mice; n = 5 for *Bmp9*KO mice. Error bars on bar charts represent \pm SEM for each group.

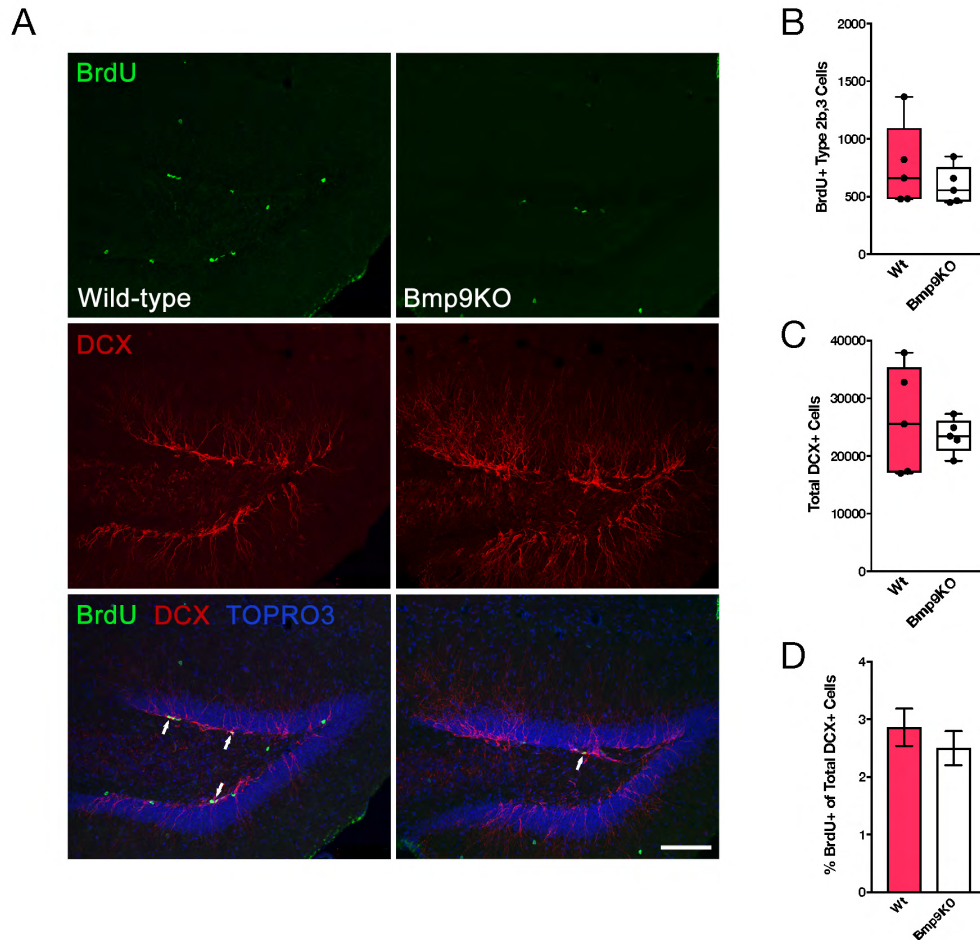
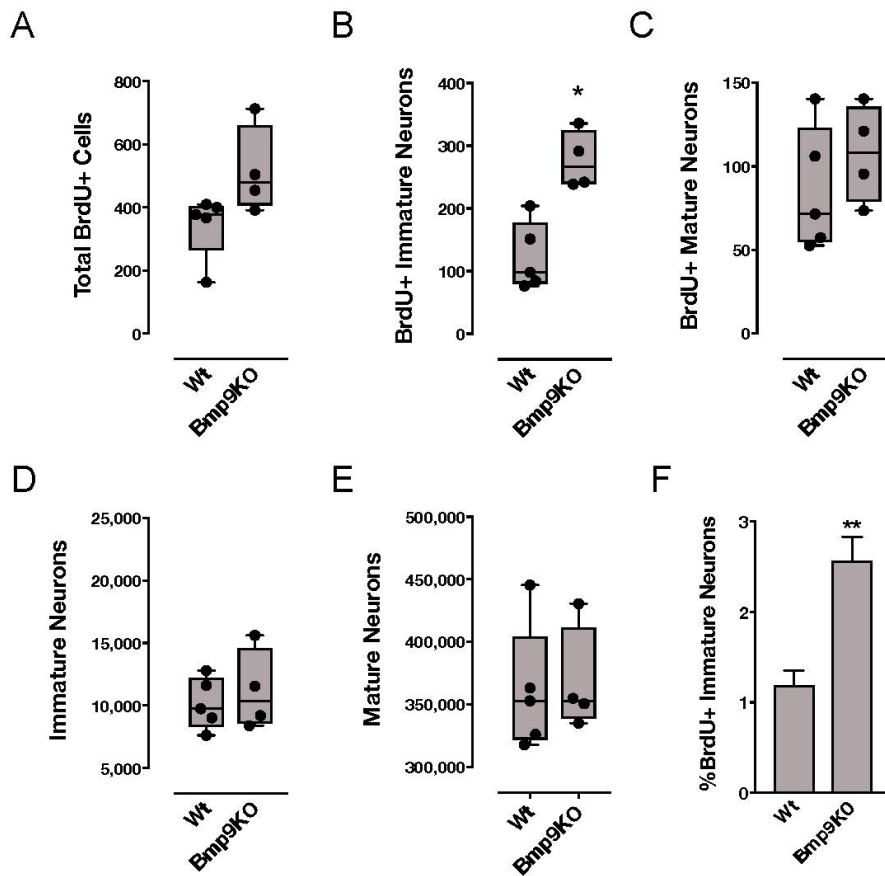


Figure 2.4. Survival of new-born neurons is increased in *Bmp9KO* mice.

(A-F) Three month old male wild-type and *Bmp9KO* mice were injected with CldU to label cells in S-phase according to the experimental paradigm in Figure A.2B. Coronal sections were immunostained for BrdU, DCX, and NeuN to evaluate survival after 23 days on the basis of label retention. Quantitative analysis using design based stereology showed (A) a marked increase in the number of label-retaining cells (BrdU+) in *Bmp9KO* mice. The total number of label-retaining cells is increased in *Bmp9KO* mice. (B) The number of label-retaining immature neurons in *Bmp9KO* mice is significantly greater than wild-type mice, but (C) the number of label-retaining mature neurons does not differ between the two groups. (D) The total number of immature neurons and (E) mature neurons is not significantly different between wild-type and *Bmp9KO* mice. (F) The percentage of label-retaining immature neurons is significantly greater in *Bmp9KO* mice. Whiskers on boxplots represent maximum and minimum values and points represent values for individual mice. n = 5 for wild-type mice; n = 4 for *Bmp9KO* mice. Error bars on bar charts represent \pm SEM for each group. *P < .05, **P < .01.



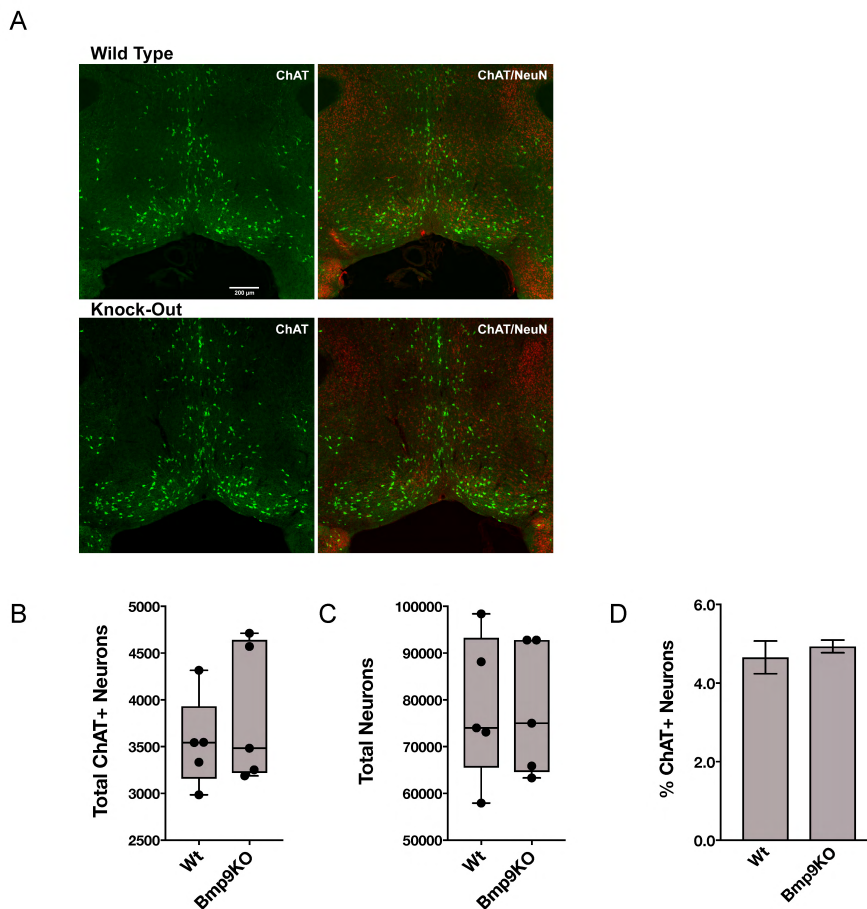
a significantly greater number of label-retaining immature neurons ($U=0$; 97.92, wild-type [$n=5$]; 266.9, *Bmp9*KO [$n=4$]; $p=.016$, Fig. 2.4B). The total number of label-retaining mature neurons, however, did not change ($U=5.5$; 71.4, wild-type [$n=5$]; 108.3, *Bmp9*KO [$n=4$]; $p=.391$, Fig. 2.4C). To assess whether the apparent increase in the survival of label-retaining immature neurons (BrdU+/DCX+/NeuN+) resulted in an increase in the total population of immature (DCX+/NeuN+) and mature (DCX-/NeuN+) neurons, we then quantified the total number of cells in each of these population. Our data indicate there is no difference in either the total population of immature ($U=9$; 9,750, wild-type [$n=5$]; 10,368, *Bmp9*KO [$n=4$]; $p=.905$, Fig. 2.4D) or mature neurons ($U=9$; 352,920, wild-type [$n=5$]; 352,800, *Bmp9*KO [$n=4$]; $p=.905$, Fig. 2.4E) between wild-type and *Bmp9*KO mice. We next determined the percentage of label-retaining immature neurons within the population of immature neurons for each group. *Bmp9*KO mice had a significantly greater percentage of label-retaining immature neurons relative to wild-type ($2.57\% \pm .263$, *Bmp9*KO [$n=4$]; $1.19\% \pm .164$, wild-type [$n=5$]; $p=.0061$, Fig. 2.4F). Taken together, these results indicate BMP9 loss-of-function enhances survival of immature neurons without expanding the population of either immature or mature neurons.

Dysregulation Of Adult Neurogenesis In *Bmp9*KO Mice Is Not Caused By An Absence Of Regional Expression Or Reduced Number Of BFCN

To determine if BMP9 is expressed in the brain, we used qPCR to assay for the presence of *Bmp9* transcripts in the anterior region, posterior region, and hippocampus of wild-type mice. As expected, *Bmp9* was detected in liver, which was used as a positive control. Conversely, the level of *Bmp9* expression within the brain was comparable to that of the hippocampus from *Bmp9*KO mice (Fig. A.4.). Although these data indicate that endogenous BMP9 does not

Figure 2.5. Endogenous BMP9 is not necessary for cholinergic support in the medial septum and diagonal band of Broca.

(A) Coronal sections from the medial septum and vertical diagonal band of Broca were immunostained for ChAT and NeuN to identify the cholinergic neurons and neurons irrespective of phenotype. (B-D) Quantitative analysis using design-based stereology showed (B) the number of cholinergic (ChAT+) neurons in basal forebrain structures do not differ between wild-type and *Bmp9*KO mice. (C) The total number of neurons, irrespective of phenotype does not differ between wild-type and *Bmp9*KO mice. (D) There is no difference between the percentage of ChAT positive neurons with respect to the entire neuronal population between wild-type and *Bmp9*KO mice. Scale bar equals 200 μ m. Whiskers on boxplots represent maximum and minimum values and points represent values for individual mice. $n = 5$ for wild-type mice; $n = 5$ for *Bmp9*KO mice. Error bars on bar charts represent \pm SEM for each group. Whiskers on boxplots represent maximum and minimum values. Error bars on charts represent \pm SEM for each group.



provide constitutive neurotrophic support to maintain BFCN at 3-4 months of age, permanent alterations to the size of the BFCN population could result from loss of BMP9-mediated support at an earlier age. To evaluate the possibility that BMP9-mediated changes in BFCN are associated with the alterations in neurogenesis observed in *Bmp9*KO mice, we quantified neurons expressing choline acetyltransferase (ChAT), a marker for cholinergic neurons, and the total number of neurons (NeuN+) in the medial septum and diagonal band of Broca (Fig. 2.5A-D). Surprisingly, the number of cholinergic neurons did not differ for wild-type (3544) and *Bmp9*KO mice (3484) ($U=11$, $p=.841$, Fig. 2.5B) and we did not detect any difference between wild-type (74000) and *Bmp9*KO mice (75023) for the total number of neurons ($U=12$, $p>.999$, Fig. 2.5C). Similarly, we did not detect any difference in proportion of cholinergic neurons (ChAT+) between the two groups (Fig. 2.5D).

DISCUSSION

BMP9 is circulating factor and well-established regulator of endothelial cell biology. During development, BMP9-ALK1 signaling prevents endothelial hypersprouting by modulating VEGF responsiveness in angiogenic endothelial cells. BMP9 continues to circulate throughout adulthood and functions to maintain vascular homeostasis (Wooderchak-Donahue et al., 2013). However, the function of endogenous BMP9 in adult tissues is not well understood. The vasculature is a crucial component of somatic stem cell niches and has an indispensable role in organ homeostasis (Rafii et al., 2016). Furthermore, experiments utilizing heterochronic parabiotics have demonstrated circulating factors can both induce and reverse age-related phenotypes (Katsimpardi et al., 2014; Villeda et al., 2011; 2014). Taken together, these findings raise the possibility BMP9 is necessary for homeostatic stem cell and precursor dynamics.

In this study, we aimed to explore this idea by examining adult hippocampal neurogenesis in *Bmp9*KO mice under basal conditions. To detect and quantify stage-specific alterations in neuronal development, we combined thymidine analog pulse-labeling, multi-label immunofluorescence, and design-based stereology. Our experimental design employed two different pulse-labeling schemes: the first was to detect changes in proliferation, whereas the second was to evaluate selective survival. This approach allowed us to identify significant differences within both precursor and post-mitotic stages of the neuronal lineage. We show proliferation is specifically decreased in the Type 2a progenitor population and an increase in the number of label-retaining immature neurons in *Bmp9*KO mice. These findings demonstrate loss of BMP9 causes dysregulation of the neurogenic process. In addition, we provide data that supports a role for BMP9 in neurogenic modulation in the absence of angiogenic stimuli and regional expression.

In vivo clonal analysis of RGL/Type 1 cells has revealed a striking amount of heterogeneity with regard to capacity for self-renewal and fate potential (Bonaguidi et al., 2011). Once activated, RGLs/Type 1 cells can divide symmetrically to expand the population, divide asymmetrically to self-renew and give rise to a progenitor of either neuronal or glial fate, or terminally differentiate into astrocytes (Bonaguidi et al., 2011; Encinas et al., 2011; Gebara et al., 2016). Whether the reservoir of RGLs/Type 1 cells is depleted during aging due to proliferative exhaustion, cellular senescence, or differentiation into astrocytes is a matter a debate and it is unlikely these scenarios are mutually exclusive. In this study, we expanded upon this idea to evaluate neurogenic versus gliogenic fate choice by assessing distribution of SOX2⁺ cells within the total population. Although we did not detect a difference in astrocytes, we show a trend toward a relatively smaller proportion of nonradial SOX2⁺/Type 2a cells that seems to come at

the cost of RGLs/Type 1 cells. It was previously shown that conditional genetic deletion of PTEN in young mice increases symmetric, expansive divisions of RGLs/Type 1 cells that subsequently differentiate into astrocytes. Consistent with the timeline of astrocyte differentiation from previous studies, there is a significant increase in the number of astrocytes and depletion of RGLs/Type 1 cells after one month (Bonaguidi et al., 2011; Encinas et al., 2011). In this context, it is conceivable we did not observe an increase in astrocyte differentiation in *Bmp9*KO mice due to an inadequate amount of time passing for such a phenotype to develop. Contrary to this idea, data from our second pulse-labeling experiment does not demonstrate a significant difference in the number of label-retaining cells after 23 days post injection that were not committed to the neurogenic lineage, i.e. putative RGLs/Type 1 cells, Type 2a cells, or astrocytes, in *Bmp9*KO mice. Instead, we show *Bmp9*KO mice have significantly more label-retaining immature neurons, which suggests proliferation of Type 2a cells might decrease due to precocious differentiation. Taken together, it is unclear whether the decrease in Type 2a cell proliferation in *Bmp9*KO mice occurs independently of RGLs/Type 1 cells, or if the combined effects of quiescence and heterogeneity prevent BMP9 loss-of-function to manifest as a population-level differences in the RGL/Type 1 cells and astrocytes at the age examined in this study. Future studies with *Bmp9*KO mice at more advanced ages would be required to resolve whether loss of BMP9 effects RGLs/Type 1 cells and astrocyte differentiation similar to ageing.

Similar to RGLs/Type 1 cells and hNSCs, Type 2a and Type 2b cells return to quiescence and are differentially reactivated according to physiological context (Bond et al., 2014; Lugert et al., 2010; 2012). Under homeostatic conditions, neurogenesis relies on hNSC to divide multiple times and proliferation of Type 2b/3 cells modulate the magnitude of neuronal output and can

take several weeks to mature (Lugert et al., 2012). By contrast, conditional genetic deletion of BMPRII in Type 2 subpopulations increases recruitment of more differentiated progenitors, which effectively shifts the starting point of neuronal development and accelerates the tempo of maturation (Bond et al., 2014). In the latter case, survival of newborn neurons is limited and presumably due to the lack of requisite stimuli for activity-dependent recruitment.

Despite a significant reduction in Type 2a cell proliferation and no compensatory increase in Type 2b/3 cell activity, we show *Bmp9*KO have comparable level of successful neuronal commitment relative to wild-type mice. We also show the number of newborn immature neurons are increased in *Bmp9*KO mice. In terms of population-based mechanisms, one possibility is that *Bmp9*KO mice have a higher frequency of Type 2 cells undergoing differentiating, asymmetric cell division at the cost of returning to a quiescent state. Overtime, precocious differentiation of quiescent Type 2a cells would be expected to destabilize the precursor pool and diminish proliferative capacity. In this scenario, age-related neurogenic decline would be potentiated as RGLs/Type 1 cells progressively lose their ability to generate hNSCs and more differentiated Type 2a cells. In the case of *Bmp9*KO mice, precocious differentiation also provides a plausible explanation for the reduction in nonradial SOX2+/Type 2a cell proliferation irrespective of RGL/Type 1 cell dynamics. Alternatively, the increase in the number of label-retaining immature neurons in *Bmp9*KO mice could be the result of protracted activity-dependent recruitment during the post-mitotic phase. Analogous to the way in which activation of quiescent Type 2 cells accelerates maturation as a population-based effect, i.e. rather than the time course of neuronal development itself, extending the period for selective survival would increase the number of label-retaining immature neurons as a function of accumulation irrespective of permanent integration into the circuitry. As retrospective

quantification of apoptotic cells is difficult due to rapid removal by microglia, we did not assay for cell survival. Therefore, whether the increase of newly generated immature neurons in *Bmp9*KO mice is the result of precursor dynamics or post-mitotic maturation remains unresolved. Though mechanistically distinct, these two scenarios are not mutually exclusive and may represent two different aspects of a coordinated response. Importantly, in the case of the latter, we would expect the total population of immature and/or mature neurons to expand as surviving cells accumulate. Elucidating these mechanisms in future studies will yield valuable insight into the niche dynamics.

BMP9 has long been associated with development and maintenance of the basal forebrain cholinergic neurons (BFCN) and acetylcholine has an established role in adult neurogenesis and maintaining hippocampal function (Cooper-Kuhn et al., 2004; Vivar et al., 2012). Previous studies have demonstrated BMP9 is sufficient to induce differentiation of BFCN during development and prevent dedifferentiation of BFCN in adult mouse models of experimental injury and disease (Lopez-Coviella et al., 2011; Mellott et al., 2014; Schnitzler et al., 2010). BFCN provide acetylcholine-mediated neuromodulation to neural precursors in the SGZ and promote survival of immature neurons (Vivar et al., 2012). Taken together, these studies provide evidence for a potential link between BMP9 function in the development and/or maintenance of the neurogenic microenvironment and adult hippocampal neurogenesis. In this study we explored this relationship by extending our stereological analysis to include quantification of cholinergic neurons in the vDBB and MS. We show the number and proportion of cholinergic neurons *Bmp9*KO mice does not differ from wild-type. Importantly, it is conceivable these neurons have altered functionality that would not be detected by the analyses conducted here. Interestingly, previous studies have shown detectable levels of BMP9 protein in the aging brain.

In the context of the vulnerable hippocampal vasculature and overlapping patterns of *Bmp9* and *Alk1* in some tissues, specifically liver and lung, it is interesting to speculate the role of BMP9 in the aging hippocampus might have dual functionality for vascular and cholinergic maintenance (Montagne et al., 2015; Park et al., 2009; Seki et al., 2003). In this scenario, regional expression of BMP9 might increase the local functionality of circulating BMP9 to overcome age-related deficits in hippocampal homeostasis. Importantly, we did not detect *Bmp9* expression in the brains of mice in this study or signs of hypervascularization in the dentate gyrus, indicating loss of brain-derived BMP9 is not related to neurogenic dysregulation at the age examined.

Taken together, the work presented in this study provides strong evidence that BMP9 modulates adult hippocampal neurogenesis. Although we do not explicitly demonstrate BMP9 functions as circulating factor, this is the most likely mechanism based on the data presented here and general knowledge of BMP9. Future studies should examine this relationship more closely. In addition, determining the functionality of increased survival of immature neurons in *Bmp9*KO mice is warranted. Furthermore, as it appears the role of BMP9 largely associates with homeostasis, the use of aging mice in future studies would likely yield more severe phenotypes.

CHAPTER 3

CONCLUSION

BMP9 is circulating factor and well-established regulator of endothelial cell biology (Bidart et al., 2011; Chen et al., 2013; David et al., 2008). During development, BMP9-ALK1 signaling prevents endothelial hypersprouting by modulating VEGF responsiveness in angiogenic endothelial cells . BMP9 continues to circulate throughout adulthood and functions to maintain vascular homeostasis (Wooderchak-Donahue et al., 2013). However, the function of endogenous BMP9 in adult tissues is not well understood. The vasculature is a crucial component of somatic stem cell niches and has an indispensable role in organ homeostasis (Rafii et al., 2016). Furthermore, experiments utilizing heterochronic parabiosis have demonstrated circulating factors can both induce and reverse age-related phenotypes (Katsimpardi et al., 2014; Villeda et al., 2011; 2014). Taken together, these findings raise the possibility BMP9 is necessary for homeostatic stem cell and precursor dynamics.

In this study, we aimed to explore this idea by examining the steady-state dynamics of adult hippocampal neurogenesis in *Bmp9*KO mice. To detect and quantify stage-specific alterations in neuronal development, we combined thymidine analog pulse-labeling, multi-label immunofluorescence, and design-based stereology. Our experimental design employed two different pulse-labeling schemes: the first was to detect changes in proliferation, whereas the

second was to evaluate selective survival. This approach allowed us to identify significant differences within both precursor and post-mitotic stages of the neuronal lineage. We show proliferation is specifically decreased in the Type 2a progenitor population, but an increase in the number of label-retaining immature neurons in *Bmp9*KO mice. These findings demonstrate loss of BMP9 causes dysregulation of the neurogenic process and define a new role for circulating BMP9.

Loss Of Bmp9 Phenocopies Aspects Of Age-Related Dysregulation Of Early Neural Precursors

Adult hippocampal neurogenesis continually produces new granule cells in the dentate gyrus. By adding new neurons to the hippocampal circuitry, this process provides the cellular basis for neuronal plasticity and is crucial for learning and adaptive behavior. The capacity to generate new neurons throughout life is fundamentally dependent on maintaining a reservoir of neural stem cells and permissive signaling within the neurogenic niche. Within the niche, endothelial cells function as intermediary signaling platforms that modulate neurogenesis in response to circulating factors and bidirectional communication with adjacent neural stem cells. Adult neurogenesis progressively decreases with age and is associated with a decrease in proliferation of neural stem cells and progenitors. On the basis of morphology, expression of endogenous markers, and lineage tracing, two types of SOX2⁺ neural precursor cells have been identified in the SGZ: i) RGLs/Type 1 cells, which have an apical process that spans the granule cell layer and express GFAP among other glial markers and ii) nonradial SOX2⁺ cells, which may arise from RGLs/Type 1 cells and typically do not express GFAP. Although both populations can shuttle between active and quiescent states, RGLs/Type 1 cells rarely enter the

cell cycle under basal conditions. By contrast, nonradial SOX2+ cells divide relatively more often and thus serve as the primary neural precursor. Sustained quiescence in the RGL/Type 1 cell pool appears to function as a mechanism to prevent exhaustive cycling and maintain proliferative capacity throughout life. BMPR1A preserves this reservoir by promoting quiescence of RGLs/Type 1 cells. Experimental inhibition of BMP signaling results in aberrant activation of RGLs/Type 1 cells and a burst in nonradial SOX2+ cell activation. In the long-term, however, the proliferative capacity of Type 1 cells is compromised, production and proliferative activity of nonradial SOX2+ neuronal output declines (Mira et al., 2010). Nonradial SOX2+ cells are not clearly delineated from Type 2a progenitors and also share characteristics with hNSCs (Lugert et al., 2010; 2012; Suh et al., 2007). Under basal conditions, RGLs/Type 1 cells are mostly quiescent, whereas hNSCs serve as the primary precursor. During aging, there is a proportionate decrease in proliferative activity in both populations. Thus, while RGLs/Type 1 cells function as a reservoir, that sustains neurogenesis, hNSCs appear to account for majority the age-associated decrease in neurogenesis (Lugert et al., 2010).

In the dentate gyrus, RGLs/Type 1 cells are in direct contact with the vasculature in the SGZ and through arborizations in the molecular layer that ensheath blood vessels (Licht and Keshet, 2015; Moss et al., 2016). Given the intimate association of RGLs/Type 1 cells with the vasculature and the role of circulating BMP9 in vascular homeostasis, we speculated RGLs/Type 1 cells might be vulnerable to dysregulation and potentiate an aging phenotype in *Bmp9*KO mice. Contrary to this hypothesis, we show loss of BMP9 results in fewer mitotically active Type 2a cells, which appears to result, in part, from a reduction in the percentage of cells that are cycling. Although the reduction in Type 2a proliferative activity observed in *Bmp9*KO mice is similar to what is observed during aging and experimental ablation of the RGLs/Type 1 reservoir

described above, we did not observe a significant difference in the number or percentage of mitotically active RGLs/Type 1 cells. In the context of aging, this might be expected as RGLs/Type 1 cells are typically quiescent under homeostatic conditions and the decline in age-related neurogenesis is progressive and primarily accounted for in the hNSC population, which phenotypically overlaps with the Type 2a cell in this study.

In vivo clonal analysis of RGL/Type 1 cells has revealed a striking amount of heterogeneity with regard to capacity for self-renewal and fate potential (Bonaguidi et al., 2011). Once activated, RGLs/Type 1 cells can divide symmetrically to expand the population, divide asymmetrically to self-renew and give rise to a progenitor of either neuronal or glial fate, or terminally differentiate into astrocytes (Bonaguidi et al., 2011; Encinas et al., 2011; Gebara et al., 2016). Whether the reservoir of RGLs/Type 1 cells is depleted during aging due to proliferative exhaustion, cellular senescence, or differentiation into astrocytes is a matter a debate and it is unlikely these scenarios are mutually exclusive. In this study, we expanded upon this idea to evaluate neurogenic versus gliogenic fate choice by assessing distribution of SOX2+ cells within the total population. Although we did not detect a difference in astrocytes, we show a trend toward a relatively smaller proportion of nonradial SOX2+/Type 2a cells that seems to come at the cost of RGLs/Type 1 cells. It was previously shown that conditional genetic deletion of PTEN in young mice increases symmetric, expansive divisions of RGLs/Type 1 cells that subsequently differentiate into astrocytes. After one month, there a significant increase in the number of astrocytes and depletion of RGLs/Type 1 cells (Bonaguidi et al., 2011). In this context, it is conceivable we did not observe an increase in astrocyte differentiation in *Bmp9KO* mice due to inadequate amount of time passing for such a phenotype to develop. Contrary to this idea, data from our second pulse-labeling experiment does not demonstrate a significant

difference in the number of label-retaining cells after 23 days post injection that were not committed to the neurogenic lineage, i.e. putative RGLs/Type 1 cells, Type 2a cells, or astrocytes, in *Bmp9*KO mice. Instead, we show *Bmp9*KO mice have significantly more label-retaining immature neurons, which suggests proliferation of Type 2a cells might decrease due to precocious differentiation. Taken together, it is unclear whether the decrease in Type 2a cell proliferation in *Bmp9*KO mice occurs independently of RGLs/Type 1 cells, or if the combined effects of quiescence and heterogeneity prevent BMP9 loss-of-function to manifest as a population-level difference in the RGL/Type 1 cells and astrocytes at the age examined in this study. Future studies with *Bmp9*KO mice at more advanced ages would be required to resolve whether loss of BMP9 effects RGLs/Type 1 cells and astrocyte differentiation similar to ageing.

Similar to RGLs/Type 1 cells and hNSCs, Type 2a and Type 2b cells return to quiescence and are differentially reactivated according to physiological context (Bond et al., 2014; Lugert et al., 2010; 2012). Under homeostatic conditions, neurogenesis relies on hNSC to divide multiple times and proliferation of Type 2b/3 cells modulate the magnitude of neuronal output and can take several weeks to mature (Lugert et al., 2012). By contrast, conditional genetic deletion of BMPRII in Type 2 cell subpopulations increases recruitment of more differentiated progenitors, which effectively shifts the starting point of neuronal development and accelerates the tempo of maturation (Bond et al., 2014). In the latter case, newborn neurons require activity dependent for synaptic integration and long-term survival.

Despite a significant reduction in Type 2a cell proliferation and no compensatory increase in Type 2b/3 cell activity, we show *Bmp9*KO have comparable level of successful neuronal commitment relative to wild-type mice. We also show a greater number of label-retaining newborn immature neurons in *Bmp9*KO mice. In terms of population-based

mechanisms, one possibility is that *Bmp9*KO mice have a higher frequency of Type 2 cells undergoing differentiating, asymmetric cell division at the cost of returning to a quiescent state. Overtime, precocious differentiation of quiescent Type 2a cells would be expected to destabilize the precursor pool and diminish proliferative capacity. In this scenario, age-related neurogenic decline would be potentiated as RGLs/Type 1 cells progressively lose their ability to generate hNSCs and more differentiated Type 2a cells. In the case of *Bmp9*KO mice, precocious differentiation also provides a plausible explanation for the reduction in nonradial SOX2+/Type 2a cell proliferation irrespective of RGL/Type 1 cell dynamics. Alternatively, the increased number of label-retaining immature neurons in *Bmp9*KO mice could be the result of protracted activity-dependent recruitment during the post-mitotic phase. Analogous to the way in which activation of quiescent Type 2 cells accelerates maturation as a population-based effect, i.e. rather than the time course of neuronal development itself, extending the period for selective survival would increase the number of label-retaining immature neurons as a function of accumulation irrespective of permanent integration into the circuitry. As retrospective quantification of apoptotic cells is difficult due to rapid removal by microglia, we did not assay for cell survival. Therefore, whether the increase of new, immature neurons in *Bmp9*KO mice is the result of precursor dynamics or post-mitotic maturation remains unresolved. Though mechanistically distinct, these two scenarios are not mutually exclusive and may represent two different aspects of a coordinated response.

In this study, we did not determine the functional relevance of the increase in label-retaining immature neurons in *Bmp9*KO mice or whether this population could be stabilized with appropriate stimuli, such as environmental enrichment. Determining the behavioral consequence of these immature neurons and the mechanism by which they arise should be

addressed in further studies. As BMP9 is not expressed in the brain, such an investigation could also increase understanding of the dynamics governing regulatory feedback and niche components.

Potential Mechanisms And Implications

The altered dynamics of adult hippocampal neurogenesis in *Bmp9*KO mice are distinct from those that result from abrogating cell autonomous BMP signaling on neural precursors (Bond et al., 2014; Mira et al., 2010). Consistent with this differences, we show *Bmp9* is not expressed in the brain of adult mice at the age neurogenesis was examined, thus precluding loss of paracrine/autocrine signaling from regionally derived BMP9 as a potential mechanism underlying the observed *Bmp9*KO phenotype. BMP9 regulates angiogenesis during development and continues to circulate at physiologically relevant levels in both adult mice and humans. Blood vessels serve as both conduits for oxygen and nutrient delivery and a source of instructive signaling from specialized endothelial cells. The hippocampal vasculature is particularly vulnerable to age-related changes, which leads to compromised BBB integrity, decreased blood perfusion, diminished adult neurogenesis, and ultimately risk for cognitive impairment (Montagne et al., 2015). Given the emerging importance of systemic regulation circulating factors in maintaining hippocampal function, it is a strong possibility BMP9 modulates adult neurogenesis through its activity as a circulating factor. However, the mechanism by which this occurs is not clear. Endothelial cells are a heterogeneous population of cells, not only with respect to the microvasculature, but also among capillary beds of different organs. The unique properties of endothelial cells in the brain have long been recognized in the context of the BBB. In addition, the role of angiocrine factors in maintaining homeostasis and

stem and progenitor cell behavior has progressively become evident (Rafii et al., 2016). Taken together, BMP9 could serve to activate niche endothelial cells for angiocrine mediated signaling or more generally to support the vasculature.

Dysregulation Of Adult Neurogenesis In *Bmp9*KO Mice Is Not Related To Basal Levels Of Angiogenesis

During development, BMP9-ALK1 signaling prevents endothelial hypersprouting by modulating VEGF responsiveness in angiogenic endothelial cells (Chen et al., 2013; Larrivée et al., 2012; Ricard et al., 2012). In certain tissues, endothelial cells maintain a proliferative state or are at least more susceptible to reactivation by angiogenic stimuli. BMP9 similarly functions as a vascular quiescence factor in adult tissues when angiogenesis is activated. ALK1 continues to be expressed in the lung and liver and genetic deletion of ALK1 in adult mice results in AVM formation in both organs under basal conditions (Park et al., 2009; Seki et al., 2003). By contrast, ALK1 expression is diminished in the vasculature of other organs where angiogenesis is only intermittently induced in response to stimuli (Seki et al., 2003). In the absence of ALK1, vascular abnormalities do not develop in the skin of adult mice unless angiogenesis is induced by injury (Park et al., 2009). Likewise, deletion of ALK1 in the brains of adult mice does not lead to AVM formation unless angiogenesis is stimulated by exogenous VEGF (Chen et al., 2014). Consistent with these findings and the experimental conditions of this study, we did not find evidence for endothelial hypersprouting in *Bmp9*KO mice. Specifically, proliferation of putative endothelial progenitor cells was comparable between *Bmp9*KO and wild-type mice. Furthermore, immunohistochemistry with CD31, an endothelial cell marker, did not reveal abnormalities in vessel morphology.

During embryonic and postnatal development, BMP9 and BMP10 are functionally redundant (Chen et al., 2013; Ricard et al., 2012). Data from early reports indicated BMP10 did not circulate in the adult in an active conformation, but evidence has recently emerged that suggests functionally active proBMP10 is detected in the serum of adult mice (Bidart et al., 2011; Jiang et al., 2016). These data raise the possibility that angiogenesis is unaffected in *Bmp9*KO mice due to genetic compensation from BMP10. While we cannot rule out this possibility, we instead propose that constitutive ALK1 signaling is not necessary to maintain vascular quiescence in mature vessels under basal conditions. Providing support for this idea, ALK1 expression is diminished in the vasculature of adult mice (Seki et al., 2003) and de novo AVM malformation requires an angiogenic stimulus in the brains of adult mice with genetic deletion of ALK (Chen et al., 2014). Furthermore, blood flow induces a physical interaction between ALK1 and Endoglin, thus suggesting endothelial cells need to be sensitized for BMP9-mediated vascular remodeling (Franco and Gerhardt, 2016).

Potential Mechanisms For BMP9 In Vascular Integrity And VEGF Signaling

The interaction between VEGF and ALK1 signaling pathways during angiogenesis raises the question of how loss of BMP9 might affect terminally differentiated endothelial cells. BMP9-ALK1 signaling has been shown to suppress VEGF expression through SMAD1 and downregulate expression of VEGFR2 downstream of HEY1 and possibly through an ID1/ID3 dependent manner (Kim et al., 2012). In addition to its function as a proangiogenic factor, VEGF increases vascular permeability, is a potent vasodilator, and negatively regulates pericyte recruitment and vessel maturation during neovascularization (Licht and Keshet, 2013). Perhaps most relevant in the context of BMP9 and vascular homeostasis, autocrine VEGF signaling is

required for the survival of quiescent, terminally differentiated endothelial cells. In contrast to mouse models where the proangiogenic function of VEGF is disrupted, genetic ablation of autocrine VEGF does not result in aberrant vascular density or patterning. Instead, adult mutant mice with a genetic deletion of VEGF specifically in the endothelial cell lineage, VEGF^{ECKO} mice, experience progressive increases in systemic endothelial apoptosis and succumb to multi-organ hemorrhage within a year (Lee et al., 2007). Though the mechanisms remains poorly understood, evidence suggests autocrine VEGF signaling is mediated by VEGFR2 signaling in an intracellular compartment, presumably through endosomal signaling complexes (Lee et al., 2007). Given the interaction between VEGF and ALK1 signaling pathways during angiogenesis, it is conceivable an analogous interaction modulates autocrine VEGF signaling to sustain viability in terminally differentiated endothelial cells (Licht and Keshet, 2013). BMP9 modulates VEGF signaling by downregulating expression of VEGFR2 downstream of HEY1 (Larrivée et al., 2012). Interestingly, BMP9 might also modulate endosomal VEGFR2 signaling by upregulating expression of EphrinB2, which interacts with VEGFR2 at the plasma membrane to mediate internalization (Kim et al., 2012; Sawamiphak et al., 2010). The interaction between EphrinB2 and VEGFR2 has yet to be investigated in a model that does not involve angiogenesis, but provides mechanistic insight for how survival of endothelial cells could be modulated by BMP9.

BMP9 Is Not Required For BFCN Development

BMP9 has long been associated with development and maintenance of the basal forebrain cholinergic neurons (BFCN) and acetylcholine has an established role in adult neurogenesis and maintaining hippocampal function. Previous studies have demonstrated BMP9 is sufficient to

induce differentiation of BFCN during development and prevent dedifferentiation of BFCN in adult mouse models of experimental injury and disease. BFCN provide acetylcholine-mediated neuromodulation to neural precursors in the SGZ and promote survival of immature neurons. Taken together, these studies provide evidence for a potential link between BMP9 function in the development and/or maintenance of the neurogenic microenvironment and adult hippocampal neurogenesis. In this study we explored this relationship by extending our stereological analysis to include quantification of cholinergic neurons in the vDBB and MS. We show the number and proportion of cholinergic neurons *Bmp9*KO mice does not differ from wild-type. Importantly, it is conceivable these neurons have altered functionality that would not be detected by the analyses conducted here. Interestingly, BMP9 is expressed in the aging brain. In the context of the vulnerable hippocampal vasculature and overlapping patterns of *Bmp9* and *Alk1* in some tissues, specifically liver and lung, it is interesting to speculate the role of BMP9 in the aging hippocampus might have dual functionality for vascular and cholinergic maintenance. In this scenario, regional expression of BMP9 might increase the local functionality of circulating BMP9 to overcome age-related deficits in hippocampal homeostasis.

Conclusions And Future Directions

Taken together, the work presented in this thesis provides strong evidence that BMP9 modulates adult hippocampal neurogenesis. Although we do not explicitly demonstrate BMP9 functions as circulating factor, this is the most likely mechanism based on the data presented here and general knowledge of BMP9. Future studies should examine this relationship more closely. In addition, determining the functionality of transient increases in immature neurons in *Bmp9*KO mice is warranted. Furthermore, as it appears the role of BMP9 largely associates with

homeostasis, the use of aging mice in future studies would likely yield more severe phenotypes.

Heterochronic parabiosis studies have demonstrated a causal link between hippocampal dysfunction and age-related changes in circulating factors. The aging systemic milieu mediates a negative influence on cognitive function in young mice, partly through an increase in inflammatory cytokines (Villeda et al., 2011). By contrast, factors in young blood were shown to rejuvenate neural vasculature, increase neurogenesis, enhance synaptic plasticity, and improve cognitive function in aging mice (Katsimpardi et al., 2014; Villeda et al., 2014). Together these findings have raised interest in manipulating ‘pro-age’ and ‘pro-youth’ factors as part of a therapeutic strategy to combat aging and induce hippocampal rejuvenation. To date, however, GDF11 is the only one ‘pro-youth’ factor to be identified and this finding is marred by controversy. Nevertheless, and regardless of translational merit, elucidating ‘pro-youth’ and ‘pro-age’ circulating factors has implications for understanding organ homeostasis and aging. Whether circulating BMP9 is an elusive ‘pro-young’ systemic factor that is capable of rejuvenation should be addressed in future studies.

APPENDIX

SUPPLEMENTARY TABLES AND FIGURES

Table A.1. Primer sequences for genotyping Bmp9KO mice.

Primer Pair	Target Description	Primer Sequence (5'-3')
PP1	Bmp9 Exon1 (Wt allele)	Fwd-TGAGTCCCATCTCCATCCTC
		Rev-ATGCAGGACCGTACCAGAAC
PP2	Bmp9 Exon1 (Wt allele)	Fwd-GGCATCTTGCTCTGAAGGAC
		Rev-GGGCAGTCAGAAAACCTCAGC
PP3	Lacz (Bmp9KO allele)	Fwd-CAGTAGTCAGCATCCTTTCC
		Rev-GCTGGCTTGGTCTGTCTGTCCTA
PP4	Neo (Bmp9KO allele)	Fwd-GCAGCCTCTGTTCCACATACTTCA
		Rev-AGTTTCTGCCTGGTTTCCTG

Table A.2. Antibodies used for multilabel immunohistochemistry.

Antibody	Dilution	Source and Catalog No.
Rat anti-BrdU BU1/75 (ICR1)	1:150	AbD Serotec OBT0030
Goat anti-SOX2 (Y-17)	1:500	Santa Cruz Biotechnology sc-1730
Chicken anti-GFAP	1:1500	Aves Labs GFAP
Goat anti-DCX (C-18)	1:500	Santa Cruz Biotechnology sc-8066
Rabbit anti-NeuN (EPR12763)	1:4000	Abcam ab177487
Goat anti-ChAT (E-7)	1:400	Santa Cruz Biotechnology sc-55557
Rat anti-Mouse CD31 (MEC 13.3)	1:400	BD Pharmingen 557355
Donkey anti-Rat Alexa Flour 488	1:500	Jackson Immunolabs 712-545-153
Donkey anti-Chicken Alexa Flour 594	1:500	Jackson Immunolabs 703-585-155
Donkey anti-Rabbit Alexa Flour 594	1:500	Jackson Immunolabs 711-585-152
Donkey anti-Goat Alexa Flour 647	1:500	Jackson Immunolabs 705-605-147
Donkey anti-Rabbit Cy3	1:500	Jackson Immunolabs 711-165-152
Donkey anti-Goat Biotin	1:500	Jackson Immunolabs 705-065-147

Table A.3. Primers used for qPCR.

Target	NCBI Identifier	Primer Sequence (5'-3')
<i>Bmp9</i>	NM_019506.4	Fwd-GCCTGCCTCCAACATCGT
		Rev-GCCCTGGTGATCTGCTCG
<i>Gapdh</i>	NM_008084, 210 bp	Fwd-GCCTCGTCCCGTAGACAAA
		Rev-TTCCCATTCTGGCCTTGAC
<i>Pecam1</i>	NM_008816.2	Fwd- TGCTCTCGAAGCCCAGTATT
		Rev- TGTGAATGTTGCTGGGTCAT

Figure A.1. Gene targeting strategy for generation of Bmp9KO mice.

(A) Bmp9 null mutants, hereafter referred to as Bmp9KO, were generated in the Transgenic Core Facility at the University of Chicago using commercially available ES cells with the Gdf2tm1(KOMP)Vlclg allele (Regeneron). Wild-type (Bmp9^{+/+}) and Bmp9KO mice for all experimental procedures were produced from (B) subsequently derived Bmp9^{+/-}. Wild-type and Bmp9KO mice were identified using genotyping primers for exon 1 (PP1), exon 2 (PP2), lacZ (PP3), and neo (PP4).

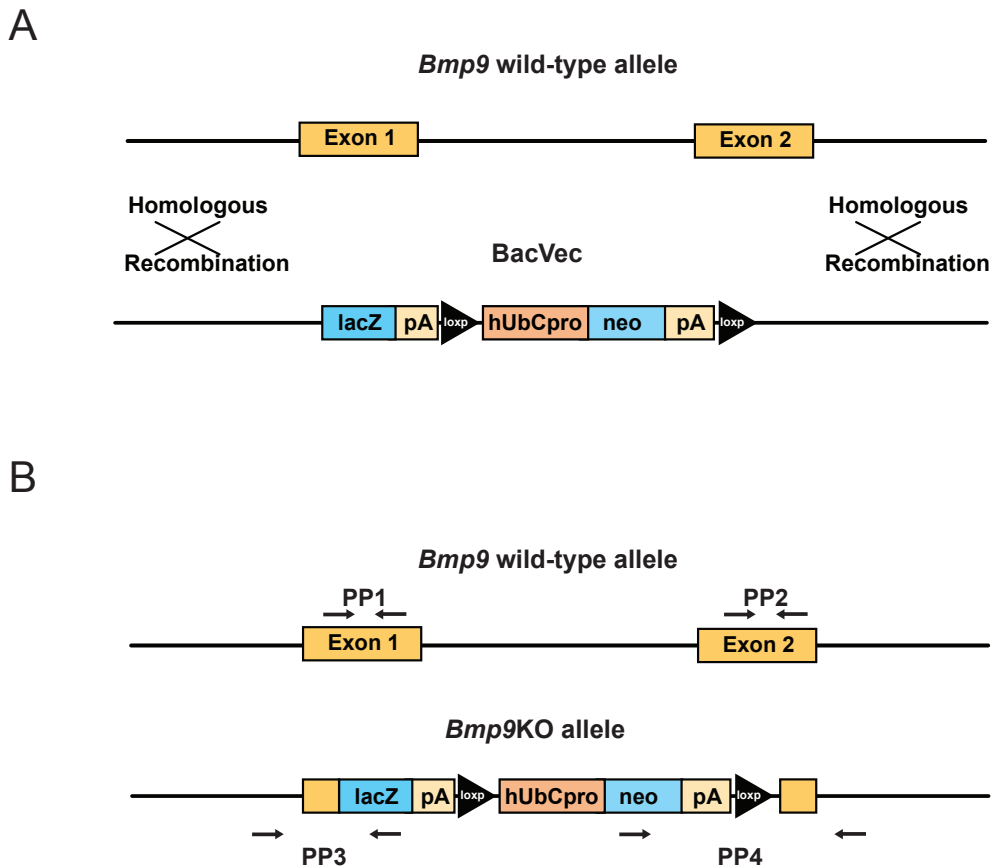


Figure A.2. Experimental design for thymidine analog pulse labeling and multi-label immunostaining.

(A) Experimental design for identification of progenitor subpopulations. Diagram depicting the injection schedule used to label proliferating cells in S phase with CldU, a halogenated thymidine analog. Mice were administered three intraperitoneal injections with two hour intervals and sacrificed two hours after the last injection. Schematic illustrating neurogenic progenitor subpopulations, mode of cell division, and markers used for multi-label immunostaining. GFAP, SOX2, and DCX are endogenous proteins differentially expressed by NSPCs. Type 1 cells express SOX2 and GFAP; Type 2a cells express SOX2, but not GFAP; Type 2b and Type 3 cells express DCX. Proliferating cells labeled with CldU are immunoreactive against antibodies for BrdU. (B) Experimental design for identification of neurogenic label-retaining cells (LRCs). Mice were administered three intraperitoneal injections with two hour intervals and sacrificed 23 days after the last injection. After 23 days, the majority of LRCs are expected to be late-stage immature neurons or morphologically mature granule cells. Schematic illustrating neurogenic LRC subpopulations that differentially express the endogenous proteins DCX and NeuN. Type 3 cells express DCX; immature neurons express DCX and NeuN; mature neurons express NeuN only. LRCs are immunoreactive against antibodies for BrdU. BMP9-mediated effects on survival and maturation are expected to alter the number and relative proportion of label-retaining, post-mitotic subpopulations in Bmp9KO mice.

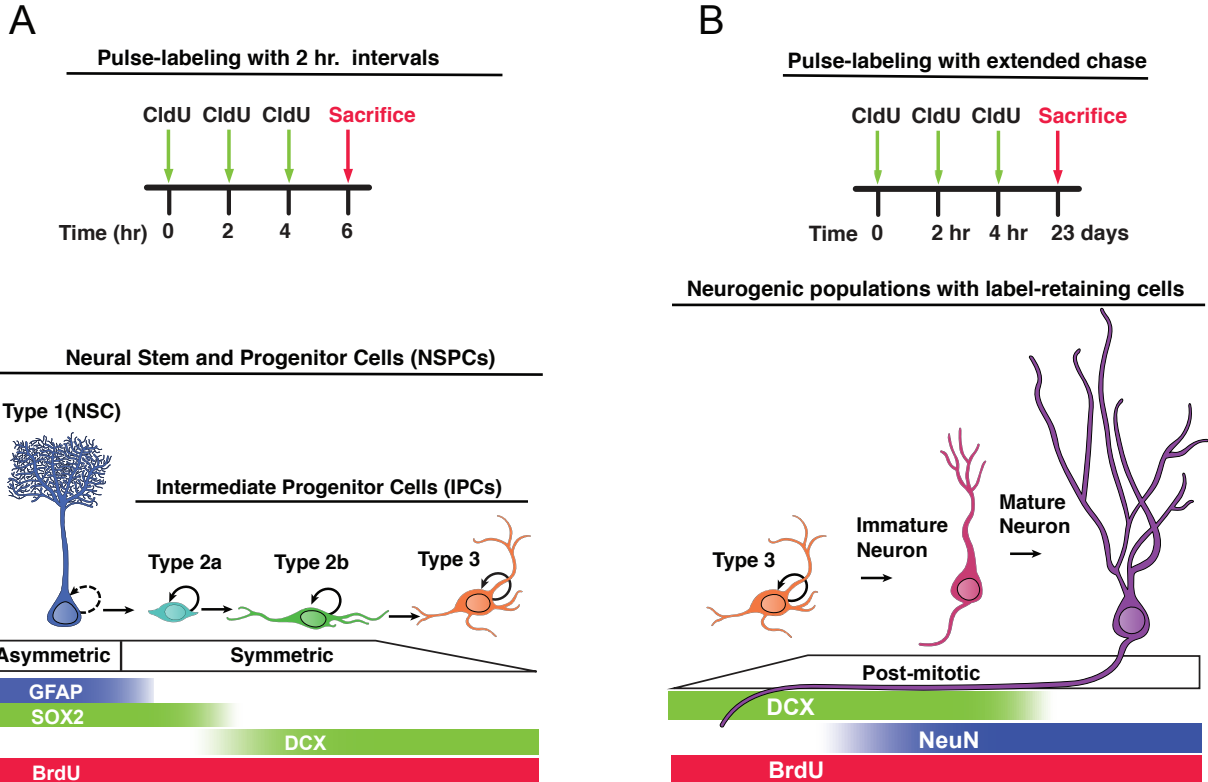


Figure A.3. Bmp9KO mice do not exhibit signs of hypervascularization.

(A) The population of unidentified BrdU+ cells, which contains endothelial cells does not differ between wild-type and Bmp9KO mice. (B) Representative image of immunostaining for CD31. Bmp9KO mice do not have apparent defects indicative of hypervascularization. Error bars represent SEM. Wild-type, n=6; Bmp9KO n=5.

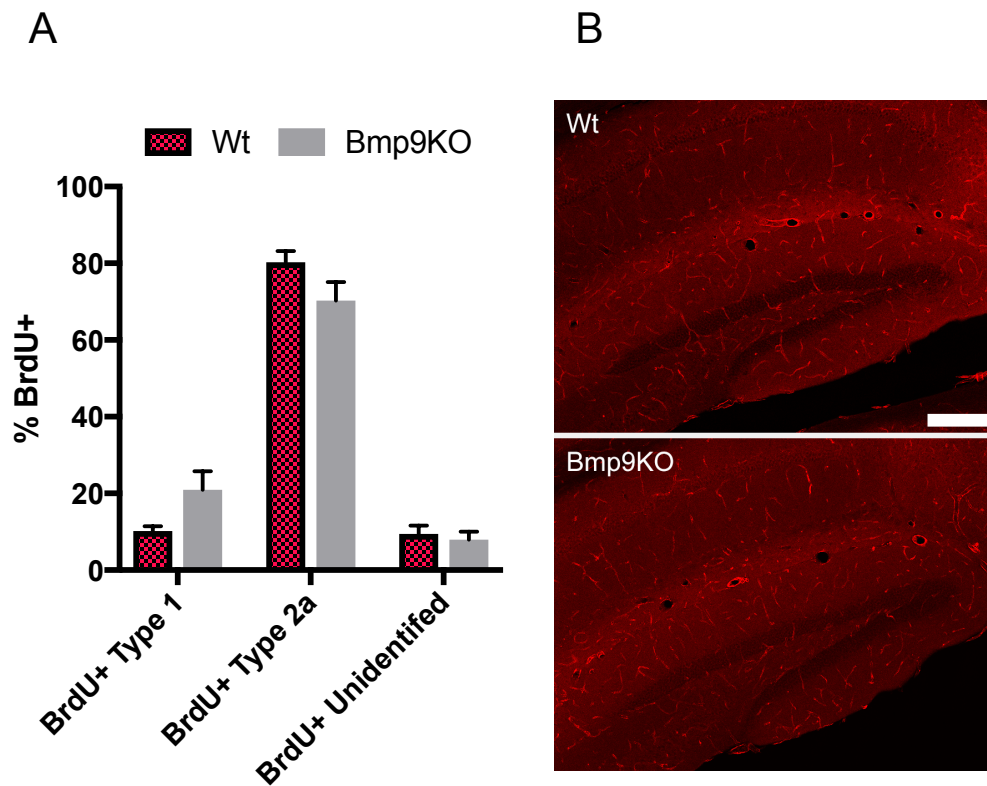
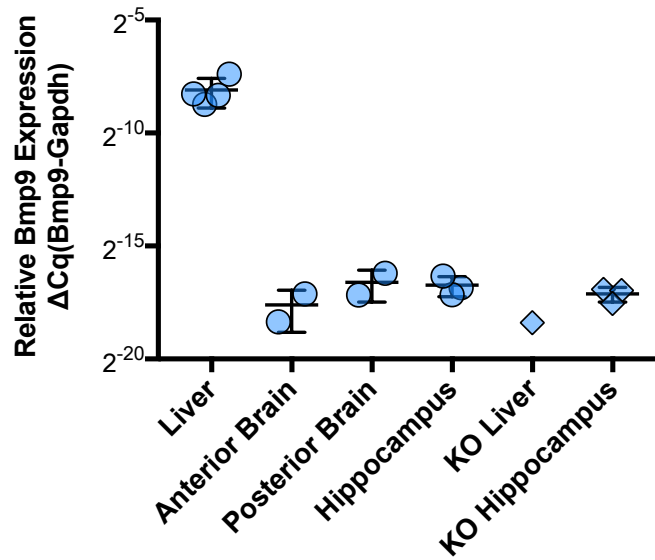


Figure A.4. *Bmp9* is not expressed in the adult male mouse brain.

Samples were collected from anterior regions, posterior regions, and hippocampi to assay for endogenous *Bmp9* expression at higher resolution. Wild-type liver was used as a positive control. Liver and hippocampi were used as negative controls. Total RNA was isolated and converted to cDNA. The cDNA was subjected to TqPCR using gene-specific primers for *Bmp9* and *Gapdh*. Relative gene expression was calculated as $\Delta Cq = Cq_{Bmp9} - Cq_{Gapdh}$.



REFERENCES

- Bidart, M., Ricard, N., Levet, S., Samson, M., Mallet, C., David, L., Subileau, M., Tillet, E., Feige, J.-J., and Bailly, S. (2011). BMP9 is produced by hepatocytes and circulates mainly in an active mature form complexed to its prodomain. *Cell. Mol. Life Sci.* *69*, 313–324.
- Bonaguidi, M.A., Song, J., Ming, G.-L., and Song, H. (2012). A unifying hypothesis on mammalian neural stem cell properties in the adult hippocampus. *Current Opinion in Neurobiology* *22*, 754–761.
- Bonaguidi, M.A., Wheeler, M.A., Shapiro, J.S., Stadel, R.P., Sun, G.J., Ming, G.-L., and Song, H. (2011). In Vivo Clonal Analysis Reveals Self-Renewing and Multipotent Adult Neural Stem Cell Characteristics. *Cell* *145*, 1142–1155.
- Bond, A.M., Peng, C.-Y., Meyers, E.A., McGuire, T., Ewaleifoh, O., and Kessler, J.A. (2014). BMP signaling regulates the tempo of adult hippocampal progenitor maturation at multiple stages of the lineage. *Stem Cells* *32*, 2201–2214.
- Burke, R.M., Norman, T.A., Haydar, T.F., Slack, B.E., Leeman, S.E., Blusztajn, J.K., and Mellott, T.J. (2013). BMP9 ameliorates amyloidosis and the cholinergic defect in a mouse model of Alzheimer's disease. *Proceedings of the National Academy of Sciences*.
- Cao, L., Jiao, X., Zuzga, D.S., Liu, Y., Fong, D.M., Young, D., and Doring, M.J. (2004). VEGF links hippocampal activity with neurogenesis, learning and memory. *Nat Genet* *36*, 827–835.
- Charytoniuk, D.A., Traiffort, E., Pinard, E., Issertial, O., Seylaz, J., and Ruat, M. (2000). Distribution of bone morphogenetic protein and bone morphogenetic protein receptor transcripts in the rodent nervous system and up-regulation of bone morphogenetic protein receptor type II in hippocampal dentate gyrus in a rat model of global cerebral ischemia. *Neuroscience* *100*, 33–43.
- Chen, H., Brady Ridgway, J., Sai, T., Lai, J., Warming, S., Chen, H., Roose-Girma, M., Zhang, G., Shou, W., and Yan, M. (2013). Context-dependent signaling defines roles of BMP9 and BMP10 in embryonic and postnatal development. *Proceedings of the National Academy of Sciences* *110*, 11887–11892.
- Chen, W., Sun, Z., Han, Z., Jun, K., Camus, M., Wankhede, M., Mao, L., Arnold, T., Young, W.L., and Su, H. (2014). De novo cerebrovascular malformation in the adult mouse after endothelial Alk1 deletion and angiogenic stimulation. *Stroke* *45*, 900–902.
- Chen, Y., Lebrun, J.J., and Vale, W. (1996). Regulation of transforming growth factor beta- and activin-induced transcription by mammalian Mad proteins. *Proc. Natl. Acad. Sci. U.S.a.* *93*, 12992–12997.
- Cooper-Kuhn, C.M., Winkler, J.R., and Kuhn, H.G. (2004). Decreased neurogenesis after cholinergic forebrain lesion in the adult rat. *J. Neurosci. Res.* *77*, 155–165.

- David, L., Mallet, C., Mazerbourg, S., Feige, J.J., and Bailly, S. (2007). Identification of BMP9 and BMP10 as functional activators of the orphan activin receptor-like kinase 1 (ALK1) in endothelial cells. *Blood* *109*, 1953–1961.
- David, L., Mallet, C., Keramidas, M., Lamandé, N., Gasc, J.-M., Dupuis-Girod, S., Plauchu, H., Feige, J.-J., and Bailly, S. (2008). Bone morphogenetic protein-9 is a circulating vascular quiescence factor. *Circ. Res.* *102*, 914–922.
- de Caestecker, M. (2004). The transforming growth factor-beta superfamily of receptors. *Cytokine & Growth Factor Reviews* *15*, 1–11.
- Doetsch, F., García-Verdugo, J.M., and Alvarez-Buylla, A. (1997). Cellular composition and three-dimensional organization of the subventricular germinal zone in the adult mammalian brain. *J. Neurosci.* *17*, 5046–5061.
- Dupuis-Girod, S., Bailly, S., and Plauchu, H. (2010). Hereditary hemorrhagic telangiectasia: from molecular biology to patient care. *J. Thromb. Haemost.* *8*, 1447–1456.
- Eaton, B.A., and Davis, G.W. (2005). LIM Kinase1 controls synaptic stability downstream of the type II BMP receptor. *Neuron* *47*, 695–708.
- Encinas, J.M., Michurina, T.V., Peunova, N., Park, J.-H., Tordo, J., Peterson, D.A., Fishell, G., Koulakov, A., and Enikolopov, G. (2011). Division-Coupled Astrocytic Differentiation and Age-Related Depletion of Neural Stem Cells in the Adult Hippocampus. *Stem Cell* *8*, 566–579.
- Fabel, K., Fabel, K., Tam, B., Kaufer, D., Baiker, A., Simmons, N., Kuo, C.J., and Palmer, T.D. (2003). VEGF is necessary for exercise-induced adult hippocampal neurogenesis. *Eur. J. Neurosci.* *18*, 2803–2812.
- Fabel, K., Wolf, S.A., Ehninger, D., Babu, H., Leal-Galicia, P., and Kempermann, G. (2009). Additive effects of physical exercise and environmental enrichment on adult hippocampal neurogenesis in mice. *Front. Neurosci.* *3*, 50.
- Fan, X., Wheatley, E.G., and Villeda, S.A. (2017). Mechanisms of Hippocampal Aging and the Potential for Rejuvenation. *Annu. Rev. Neurosci.* *40*, 251–272.
- Feng, X.H., and Derynck, R. (1997). A kinase subdomain of transforming growth factor-beta (TGF-beta) type I receptor determines the TGF-beta intracellular signaling specificity. *The EMBO Journal* *16*, 3912–3923.
- Foletta, V.C., Moussi, N., Sarmiere, P.D., Bamberg, J.R., and Bernard, O. (2004). LIM kinase 1, a key regulator of actin dynamics, is widely expressed in embryonic and adult tissues. *Exp. Cell Res.* *294*, 392–405.
- Franco, C.A., and Gerhardt, H. (2016). Blood flow boosts BMP signaling to keep vessels in shape. *J. Cell Biol.* *214*, 793–795.
- Gage, F.H. (2000). Mammalian neural stem cells. *Science* *287*, 1433–1438.

- Ge, S., Goh, E.L.K., Sailor, K.A., Kitabatake, Y., Ming, G.-L., and Song, H. (2006). GABA regulates synaptic integration of newly generated neurons in the adult brain. *Nature* *439*, 589–593.
- Ge, S., Yang, C.-H., Hsu, K.-S., Ming, G.-L., and Song, H. (2007). A critical period for enhanced synaptic plasticity in newly generated neurons of the adult brain. *Neuron* *54*, 559–566.
- Gebara, E., Bonaguidi, M.A., Beckervordersandforth, R., Sultan, S., Udry, F., Gijs, P.-J., Lie, D.-C., Ming, G.-L., Song, H., and Toni, N. (2016). Heterogeneity of Radial Glia-Like Cells in the Adult Hippocampus. *Stem Cells* *34*, 997–1010.
- Gobeske, K.T., Das, S., Bonaguidi, M.A., Weiss, C., Radulovic, J., Disterhoft, J.F., and Kessler, J.A. (2009). BMP signaling mediates effects of exercise on hippocampal neurogenesis and cognition in mice. *PLoS ONE* *4*, e7506.
- Goldman, S.A., and Chen, Z. (2011). Perivascular instruction of cell genesis and fate in the adult brain. *Nat Neurosci* *14*, 1382–1389.
- Gonçalves, J.T., Schafer, S.T., and Gage, F.H. (2016). Adult Neurogenesis in the Hippocampus: From Stem Cells to Behavior. *Cell* *167*, 897–914.
- Götz, M., Nakafuku, M., and Petrik, D. (2016). Neurogenesis in the Developing and Adult Brain-Similarities and Key Differences. *Cold Spring Harbor Perspectives in Biology* *8*, a018853.
- Graff, J.M., Bansal, A., and Melton, D.A. (1996). Xenopus Mad proteins transduce distinct subsets of signals for the TGF beta superfamily. *Cell* *85*, 479–487.
- Harradine, K.A., and Akhurst, R.J. (2006). Mutations of TGFbeta signaling molecules in human disease. *Ann. Med.* *38*, 403–414.
- Hartung, A., Bitton-Worms, K., Rechtman, M.M., Wenzel, V., Boergermann, J.H., Hassel, S., Henis, Y.I., and Knaus, P. (2006). Different routes of bone morphogenic protein (BMP) receptor endocytosis influence BMP signaling. *Mol. Cell. Biol.* *26*, 7791–7805.
- Heinecke, K., Seher, A., Schmitz, W., Mueller, T.D., Sebald, W., and Nickel, J. (2009). Receptor oligomerization and beyond: a case study in bone morphogenetic proteins. *BMC Biol.* *7*, 59.
- Hodge, R.D., Kowalczyk, T.D., Wolf, S.A., Encinas, J.M., Rippey, C., Enikolopov, G., Kempermann, G., and Hevner, R.F. (2008). Intermediate Progenitors in Adult Hippocampal Neurogenesis: Tbr2 Expression and Coordinate Regulation of Neuronal Output. *Journal of Neuroscience* *28*, 3707–3717.
- Hodge, R.D., Nelson, B.R., Kahoud, R.J., Yang, R., Mussar, K.E., Reiner, S.L., and Hevner, R.F. (2012). Tbr2 is essential for hippocampal lineage progression from neural stem cells to intermediate progenitors and neurons. *Journal of Neuroscience* *32*, 6275–6287.
- Horbelt, D., Denkis, A., and Knaus, P. (2012). A portrait of Transforming Growth Factor β superfamily signalling: Background matters. *Int. J. Biochem. Cell Biol.* *44*, 469–474.

- Jiang, H., Salmon, R.M., Upton, P.D., Wei, Z., Lawera, A., Davenport, A.P., Morrell, N.W., and Li, W. (2016). The Prodomain-bound Form of Bone Morphogenetic Protein 10 Is Biologically Active on Endothelial Cells. *Journal of Biological Chemistry* *291*, 2954–2966.
- Katsimpardi, L., Litterman, N.K., Schein, P.A., Miller, C.M., Loffredo, F.S., Wojtkiewicz, G.R., Chen, J.W., Lee, R.T., Wagers, A.J., and Rubin, L.L. (2014). Vascular and Neurogenic Rejuvenation of the Aging Mouse Brain by Young Systemic Factors. *Science* *344*, 630–634.
- Kempermann, G., Kuhn, H.G., and Gage, F.H. (1997). More hippocampal neurons in adult mice living in an enriched environment. *Nature* *386*, 493–495.
- Kempermann, G. (2015). Activity Dependency and Aging in the Regulation of Adult Neurogenesis. *Cold Spring Harbor Perspectives in Biology* *7*, a018929.
- Kempermann, G., Jessberger, S., Steiner, B., and Kronenberg, G. (2004). Milestones of neuronal development in the adult hippocampus. *Trends in Neurosciences* *27*, 447–452.
- Kempermann, G., Song, H., and Gage, F.H. (2015). Neurogenesis in the Adult Hippocampus. *Cold Spring Harbor Perspectives in Biology* *7*, a018812–a018816.
- Kim, J.-H., Peacock, M.R., George, S.C., and Hughes, C.C.W. (2012). BMP9 induces EphrinB2 expression in endothelial cells through an Alk1-BMPRII/ActRII-ID1/ID3-dependent pathway: implications for hereditary hemorrhagic telangiectasia type II. *Angiogenesis* *15*, 497–509.
- Kretschmar, M., Liu, F., Hata, A., Doody, J., and Massagué, J. (1997). The TGF-beta family mediator Smad1 is phosphorylated directly and activated functionally by the BMP receptor kinase. *Genes & Development* *11*, 984–995.
- Lagace, D.C., Whitman, M.C., Noonan, M.A., Ables, J.L., DeCarolis, N.A., Arguello, A.A., Donovan, M.H., Fischer, S.J., Farnbauch, L.A., Beech, R.D., et al. (2007). Dynamic contribution of nestin-expressing stem cells to adult neurogenesis. *Journal of Neuroscience* *27*, 12623–12629.
- Larrivé, B., Prahst, C., Gordon, E., del Toro, R., Mathivet, T., Duarte, A., Simons, M., and Eichmann, A. (2012). ALK1 Signaling Inhibits Angiogenesis by Cooperating with the Notch Pathway. *Developmental Cell* *22*, 489–500.
- Lee, S., Chen, T.T., Barber, C.L., Jordan, M.C., Murdock, J., Desai, S., Ferrara, N., Nagy, A., Roos, K.P., and Iruela-Arispe, M.L. (2007). Autocrine VEGF signaling is required for vascular homeostasis. *Cell* *130*, 691–703.
- Licht, T., and Keshet, E. (2013). Delineating multiple functions of VEGF-A in the adult brain. *Cell. Mol. Life Sci.* *70*, 1727–1737.
- Licht, T., and Keshet, E. (2015). The vascular niche in adult neurogenesis. *Mech. Dev.* *138 Pt 1*, 56–62.
- Liu, F., Hata, A., Baker, J.C., Doody, J., Cárcamo, J., Harland, R.M., and Massagué, J. (1996). A human Mad protein acting as a BMP-regulated transcriptional activator. *Nature* *381*, 620–623.

Lopez-Coviella, I. (2000). Induction and Maintenance of the Neuronal Cholinergic Phenotype in the Central Nervous System by BMP-9. *Science* 289, 313–316.

Lopez-Coviella, I., Follettie, M.T., Mellott, T.J., Kovacheva, V.P., Slack, B.E., Diesl, V., Berse, B., Thies, R.S., and Blusztajn, J.K. (2005). Bone morphogenetic protein 9 induces the transcriptome of basal forebrain cholinergic neurons. *Proc. Natl. Acad. Sci. U.S.A.* 102, 6984–6989.

Lopez-Coviella, I., Mellott, T.J., Schnitzler, A.C., and Blusztajn, J.K. (2011). BMP9 Protects Septal Neurons from Axotomy-Evoked Loss of Cholinergic Phenotype. *PLoS ONE* 6, e21166–e21168.

Lugert, S., Basak, O., Knuckles, P., Haussler, U., Fabel, K., Götz, M., Haas, C.A., Kempermann, G., Taylor, V., and Giachino, C. (2010). Quiescent and Active Hippocampal Neural Stem Cells with Distinct Morphologies Respond Selectively to Physiological and Pathological Stimuli and Aging. *Stem Cell* 6, 445–456.

Lugert, S., Vogt, M., Tchorz, J.S., Müller, M., Giachino, C., and Taylor, V. (2012). Homeostatic neurogenesis in the adult hippocampus does not involve amplification of *Ascl1*(high) intermediate progenitors. *Nature Communications* 3, 670.

Markakis, E.A., and Gage, F.H. (1999). Adult-generated neurons in the dentate gyrus send axonal projections to field CA3 and are surrounded by synaptic vesicles. *J. Comp. Neurol.* 406, 449–460.

Matsuura, I., Endo, M., Hata, K., Kubo, T., Yamaguchi, A., Saeki, N., and Yamashita, T. (2007). BMP inhibits neurite growth by a mechanism dependent on LIM-kinase. *Biochemical and Biophysical Research Communications* 360, 868–873.

Mellott, T.J., Pender, S.M., Burke, R.M., Langley, E.A., and Blusztajn, J.K. (2014). IGF2 Ameliorates Amyloidosis, Increases Cholinergic Marker Expression and Raises BMP9 and Neurotrophin Levels in the Hippocampus of the APP^{swe}PS1^{dE9} Alzheimer's Disease Model Mice. *PLoS ONE* 9, e94287.

Ming, G.-L., and Song, H. (2011). Adult Neurogenesis in the Mammalian Brain: Significant Answers and Significant Questions. *Neuron* 70, 687–702.

Mira, H., Andreu, Z., Suh, H., Lie, D.C., Jessberger, S., Consiglio, A., Emeterio, J.S., Hortigüela, R., Marqués-Torrejón, M.Á., Nakashima, K., et al. (2010). Signaling through BMPR-IA Regulates Quiescence and Long-Term Activity of Neural Stem Cells in the Adult Hippocampus. *Stem Cell* 7, 78–89.

Montagne, A., Barnes, S.R., Sweeney, M.D., Halliday, M.R., Sagare, A.P., Zhao, Z., Toga, A.W., Jacobs, R.E., Liu, C.Y., Amezcua, L., et al. (2015). Blood-brain barrier breakdown in the aging human hippocampus. *Neuron* 85, 296–302.

Moss, J., Gebara, E., Bushong, E.A., Sánchez-Pascual, I., O’Laoi, R., M’Ghari, El, I., Kocher-Braissant, J., Ellisman, M.H., and Toni, N. (2016). Fine processes of Nestin-GFP-positive radial

- glia-like stem cells in the adult dentate gyrus ensheath local synapses and vasculature. *Proc. Natl. Acad. Sci. U.S.A.* *113*, E2536–E2545.
- Mueller, T.D. (2015). Mechanisms of BMP-Receptor Interaction and Activation. *Vitam. Horm.* *99*, 1–61.
- Mueller, T.D., and Nickel, J. (2012). Promiscuity and specificity in BMP receptor activation. *FEBS Letters* *586*, 1846–1859.
- Nakao, A., Imamura, T., Souchelnytskyi, S., Kawabata, M., Ishisaki, A., Oeda, E., Tamaki, K., Hanai, J., Heldin, C.H., Miyazono, K., et al. (1997). TGF-beta receptor-mediated signalling through Smad2, Smad3 and Smad4. *The EMBO Journal* *16*, 5353–5362.
- Nakayama, M., Nakayama, A., van Lessen, M., Yamamoto, H., Hoffmann, S., Drexler, H.C.A., Itoh, N., Hirose, T., Breier, G., Vestweber, D., et al. (2013). Spatial regulation of VEGF receptor endocytosis in angiogenesis. *Nat Cell Biol* *15*, 249–260.
- Nohe, A., Hassel, S., Ehrlich, M., Neubauer, F., Sebald, W., Henis, Y.I., and Knaus, P. (2002). The mode of bone morphogenetic protein (BMP) receptor oligomerization determines different BMP-2 signaling pathways. *J. Biol. Chem.* *277*, 5330–5338.
- Orlova, V.V., Liu, Z., Goumans, M.J., and Dijke, ten, P. (2011). Controlling angiogenesis by two unique TGF- β type I receptor signaling pathways. *Histol. Histopathol.* *26*, 1219–1230.
- Palmer, T.D., Willhoite, A.R., and Gage, F.H. (2000). Vascular niche for adult hippocampal neurogenesis. *J. Comp. Neurol.* *425*, 479–494.
- Park, S.O., Wankhede, M., Lee, Y.J., Choi, E.-J., Fliess, N., Choe, S.-W., Oh, S.-H., Walter, G., Raizada, M.K., Sorg, B.S., et al. (2009). Real-time imaging of de novo arteriovenous malformation in a mouse model of hereditary hemorrhagic telangiectasia. *J. Clin. Invest.* *119*, 3487–3496.
- Plümpe, T., Ehninger, D., Steiner, B., Klempin, F., Jessberger, S., Brandt, M., Römer, B., Rodriguez, G.R., Kronenberg, G., and Kempermann, G. (2006). Variability of doublecortin-associated dendrite maturation in adult hippocampal neurogenesis is independent of the regulation of precursor cell proliferation. *BMC Neuroscience* *7*, 77.
- Rafii, S., Butler, J.M., and Ding, B.-S. (2016). Angiocrine functions of organ-specific endothelial cells. *Nature* *529*, 316–325.
- Rebbapragada, A., Benchabane, H., Wrana, J.L., Celeste, A.J., and Attisano, L. (2003). Myostatin signals through a transforming growth factor beta-like signaling pathway to block adipogenesis. *Mol. Cell. Biol.* *23*, 7230–7242.
- Ricard, N., Bidart, M., Mallet, C., Lesca, G., Giraud, S., Prudent, R., Feige, J.J., and Bailly, S. (2010). Functional analysis of the BMP9 response of ALK1 mutants from HHT2 patients: a diagnostic tool for novel ACVRL1 mutations. *Blood* *116*, 1604–1612.

- Ricard, N., Ciais, D., Levet, S., Subileau, M., Mallet, C., Zimmers, T.A., Lee, S.-J., Bidart, M., Feige, J.-J., and Bailly, S. (2012). BMP9 and BMP10 are critical for postnatal retinal vascular remodeling. *Blood* *119*, 6162–6171.
- Rider, C.C., and Mulloy, B. (2010). Bone morphogenetic protein and growth differentiation factor cytokine families and their protein antagonists. *Biochem. J.* *429*, 1–12.
- Saito, T., Bokhove, M., Croci, R., Zamora-Caballero, S., Han, L., Letarte, M., de Sanctis, D., and Jovine, L. (2017). Structural Basis of the Human Endoglin-BMP9 Interaction: Insights into BMP Signaling and HHT1. *Cell Rep* *19*, 1917–1928.
- Saitoh, M., Nishitoh, H., Amagasa, T., Miyazono, K., Takagi, M., and Ichijo, H. (1996). Identification of important regions in the cytoplasmic juxtamembrane domain of type I receptor that separate signaling pathways of transforming growth factor-beta. *J. Biol. Chem.* *271*, 2769–2775.
- Sawamiphak, S., Seidel, S., Essmann, C.L., Wilkinson, G.A., Pitulescu, M.E., Acker, T., and Acker-Palmer, A. (2010). Ephrin-B2 regulates VEGFR2 function in developmental and tumour angiogenesis. *Nature* *465*, 487–491.
- Schnitzler, A.C., Mellott, T.J., Lopez-Coviella, I., Tallini, Y.N., Kotlikoff, M.I., Follettie, M.T., and Blusztajn, J.K. (2010). BMP9 (bone morphogenetic protein 9) induces NGF as an autocrine/paracrine cholinergic trophic factor in developing basal forebrain neurons. *Journal of Neuroscience* *30*, 8221–8228.
- Seemann, P., Brehm, A., König, J., Reissner, C., Stricker, S., Kuss, P., Haupt, J., Renninger, S., Nickel, J., Sebald, W., et al. (2009). Mutations in GDF5 reveal a key residue mediating BMP inhibition by NOGGIN. *PLoS Genet* *5*, e1000747.
- Seki, T., Yun, J., and Oh, S.P. (2003). Arterial endothelium-specific activin receptor-like kinase 1 expression suggests its role in arterialization and vascular remodeling. *Circ. Res.* *93*, 682–689.
- Seri, B., García-Verdugo, J.M., McEwen, B.S., and Alvarez-Buylla, A. (2001). Astrocytes give rise to new neurons in the adult mammalian hippocampus. *Journal of Neuroscience* *21*, 7153–7160.
- Seri, B., Garcia-Verdugo, J.M., Collado-Morente, L., McEwen, B.S., and Alvarez-Buylla, A. (2004). Cell types, lineage, and architecture of the germinal zone in the adult dentate gyrus. *J. Comp. Neurol.* *478*, 359–378.
- Shao, E.S., Lin, L., Yao, Y., and Boström, K.I. (2009). Expression of vascular endothelial growth factor is coordinately regulated by the activin-like kinase receptors 1 and 5 in endothelial cells. *Blood* *114*, 2197–2206.
- Shovlin, C.L., Hughes, J.M., Scott, J., Seidman, C.E., and Seidman, J.G. (1997). Characterization of endoglin and identification of novel mutations in hereditary hemorrhagic telangiectasia. *The American Journal of Human Genetics* *61*, 68–79.

- Sierra, A., Encinas, J.M., Deudero, J.J.P., Chancey, J.H., Enikolopov, G., Overstreet-Wadiche, L.S., Tsirka, S.E., and Maletic-Savatic, M. (2010). Microglia shape adult hippocampal neurogenesis through apoptosis-coupled phagocytosis. *Cell Stem Cell* 7, 483–495.
- Söderström, S., Bengtsson, H., and Ebendal, T. (1996). Expression of serine/threonine kinase receptors including the bone morphogenetic factor type II receptor in the developing and adult rat brain. *Cell Tissue Res* 286, 269–279.
- Suh, H., Consiglio, A., Ray, J., Sawai, T., D'Amour, K.A., and Gage, F.H. (2007). In vivo fate analysis reveals the multipotent and self-renewal capacities of Sox2⁺ neural stem cells in the adult hippocampus. *Stem Cell* 1, 515–528.
- Tashiro, A., Makino, H., and Gage, F.H. (2007). Experience-specific functional modification of the dentate gyrus through adult neurogenesis: a critical period during an immature stage. *Journal of Neuroscience* 27, 3252–3259.
- Tashiro, A., Sandler, V.M., Toni, N., Zhao, C., and Gage, F.H. (2006). NMDA-receptor-mediated, cell-specific integration of new neurons in adult dentate gyrus. *Nature* 442, 929–933.
- Taylor, S., Wakem, M., Dijkman, G., Alsarraj, M., and Nguyen, M. (2010). A practical approach to RT-qPCR-Publishing data that conform to the MIQE guidelines. *Methods* 50, S1–S5.
- Toni, N., Laplagne, D.A., Zhao, C., Lombardi, G., Ribak, C.E., Gage, F.H., and Schinder, A.F. (2008). Neurons born in the adult dentate gyrus form functional synapses with target cells. *Nat Neurosci* 11, 901–907.
- Townson, S.A., Martinez-Hackert, E., Greppi, C., Lowden, P., Sako, D., Liu, J., Ucran, J.A., Liharska, K., Underwood, K.W., Seehra, J., et al. (2012). Specificity and structure of a high affinity activin receptor-like kinase 1 (ALK1) signaling complex. *Journal of Biological Chemistry* 287, 27313–27325.
- van Praag, H., Kempermann, G., and Gage, F.H. (1999). Running increases cell proliferation and neurogenesis in the adult mouse dentate gyrus. *Nat Neurosci* 2, 266–270.
- van Praag, H., Schinder, A.F., Christie, B.R., Toni, N., Palmer, T.D., and Gage, F.H. (2002). Functional neurogenesis in the adult hippocampus. *Nature* 415, 1030–1034.
- Villeda, S.A., Luo, J., Mosher, K.I., Zou, B., Britschgi, M., Bieri, G., Stan, T.M., Fainberg, N., Ding, Z., Eggel, A., et al. (2011). The ageing systemic milieu negatively regulates neurogenesis and cognitive function. *Nature* 477, 90–94.
- Villeda, S.A., Plambeck, K.E., Middeldorp, J., Castellano, J.M., Mosher, K.I., Luo, J., Smith, L.K., Bieri, G., Lin, K., Berdnik, D., et al. (2014). Young blood reverses age-related impairments in cognitive function and synaptic plasticity in mice. *Nat. Med.* 20, 659–663.
- Vivar, C., Potter, M.C., and van Praag, H. (2013). All about running: synaptic plasticity, growth factors and adult hippocampal neurogenesis. *Curr Top Behav Neurosci* 15, 189–210.

- Vivar, C., Potter, M.C., Choi, J., Lee, J.-Y., Stringer, T.P., Callaway, E.M., Gage, F.H., Suh, H., and van Praag, H. (2012). *Nature Communications* 3, 1107–1111.
- Wang, Y., Nakayama, M., Pitulescu, M.E., Schmidt, T.S., Bochenek, M.L., Sakakibara, A., Adams, S., Davy, A., Deutsch, U., Lüthi, U., et al. (2010). Ephrin-B2 controls VEGF-induced angiogenesis and lymphangiogenesis. *Nature* 465, 483–486.
- Wieser, R., Wrana, J.L., and Massagué, J. (1995). GS domain mutations that constitutively activate T beta R-I, the downstream signaling component in the TGF-beta receptor complex. *The EMBO Journal* 14, 2199–2208.
- Willis, S.A., Zimmerman, C.M., Li, L.I., and Mathews, L.S. (1996). Formation and activation by phosphorylation of activin receptor complexes. *Mol. Endocrinol.* 10, 367–379.
- Wooderchak-Donahue, W.L., McDonald, J., O'Fallon, B., Upton, P.D., Li, W., Roman, B.L., Young, S., Plant, P., Fülöp, G.T., Langa, C., et al. (2013). BMP9 mutations cause a vascular-anomaly syndrome with phenotypic overlap with hereditary hemorrhagic telangiectasia. *Am. J. Hum. Genet.* 93, 530–537.
- Wrana, J.L., Attisano, L., Wieser, R., Ventura, F., and Massagué, J. (1994). Mechanism of activation of the TGF-beta receptor. *Nature* 370, 341–347.
- Yamaguchi, K., Nagai, S., Ninomiya-Tsuji, J., Nishita, M., Tamai, K., Irie, K., Ueno, N., Nishida, E., Shibuya, H., and Matsumoto, K. (1999). XIAP, a cellular member of the inhibitor of apoptosis protein family, links the receptors to TAB1-TAK1 in the BMP signaling pathway. *The EMBO Journal* 18, 179–187.
- Yamashita, H., Dijke, ten, P., Franzén, P., Miyazono, K., and Heldin, C.H. (1994). Formation of hetero-oligomeric complexes of type I and type II receptors for transforming growth factor-beta. *J. Biol. Chem.* 269, 20172–20178.
- Yao, Y., Jumabay, M., Ly, A., Radparvar, M., Wang, A.H., Abdmaulen, R., and Boström, K.I. (2012). Crossveinless 2 regulates bone morphogenetic protein 9 in human and mouse vascular endothelium. *Blood* 119, 5037–5047.
- Zacchigna, S., Lambrechts, D., and Carmeliet, P. (2008). Neurovascular signalling defects in neurodegeneration. *Nat Rev Neurosci* 9, 169–181.
- Zhang, Y., Feng, X., We, R., and Derynck, R. (1996). Receptor-associated Mad homologues synergize as effectors of the TGF-beta response. *Nature* 383, 168–172.
- Zhao, C., Teng, E.M., Summers, R.G., Ming, G.-L., and Gage, F.H. (2006). Distinct morphological stages of dentate granule neuron maturation in the adult mouse hippocampus. *Journal of Neuroscience* 26, 3–11.